

Table 1. Surface Characteristics of the Commercial Activated Carbons (NORIT) Used in This Study

	Activated Carbons		
	AC-1 (ROX 0.8)	AC-2 (PAC 200)	AC-3 (Darco 12 × 40)
S_{BET} (m ² /g)	1024 (1100*)	1346	616 (650*)
$V_{0.99}$ (mL/g)	0.625	0.713	0.637
$V_{\alpha, \text{mic}}$ (<0.8 nm) (mL/g)	0.152	0.139	0.085
mean pore diam (nm)	2.4	2.1	4.1
iodine number	960 (1000*)	1060 (900*)	635 (600*)
methylene blue (g/(100 g))	22.3 (22*)	47.0	17.4
pHpzc	8.0	8.7	
	Surface Groups (mequiv/g)		
carboxyl	0.2	0.3	0.4
phenolic	4.2	3.0	0.8
lactone	0.1	0.0	0.5
carbonyl	0.5	4.6	0.9
basic groups	2.1	1.2	0.5

* Table data provided by NORIT.

impurities from carbohydrate products, having been tested for the detoxification of xylose solutions from the acid hydrolysis of eucalyptus wood before fermentation to xylitol,¹⁵ for the recovery of xylitol from the fermented hydrolyzates of sugarcane bagasse,¹⁶ for the selective recovery of ferulic acid from hydrolyzates of sugar-beet pulps,^{17,18} for the separation of maltopentaose from other malto-oligosaccharides,¹⁹ and for the decolorization of sugar solutions²⁰ and xylo-oligosaccharides.²¹ However, so far, there has been no detailed study of the performance of activated carbons for the removal of lignin-derived impurities from crude xylo-oligosaccharide solutions or of the characteristics of the carbons that favor the selective adsorption of lignin-related impurities.

In this paper, we study the performance of three commercial activated carbons for the purification of xylo-oligosaccharides by the selective adsorption of lignin-derived compounds and other impurities. Equilibrium experiments were conducted to obtain the adsorption isotherms, and the results were correlated with the physicochemical properties of the carbons. Continuous adsorption experiments were conducted in a packed-bed column to obtain the breakthrough curves for xylo-oligosaccharides and lignin-derived impurities.

Experimental Section

Materials. Samples of three commercial activated carbons supplied by NORIT (NORIT, the Netherlands) were tested for the purification of the xylo-oligosaccharides: ROX 0.8 (AC-1), PAC200 (AC-2), and Darco 12 × 40 (AC-3). ROX 0.8 is an extruded granular activated carbon used for decoloring starch hydrolyzates and sugars. PAC200 is a powdered carbon used for removing taste, odor, and color from water and industrial process applications. The 12 × 40 carbon is a general-purpose granular carbon grade used in a variety of applications including the purification of fine chemicals and food. For the equilibrium experiments, ROX 0.8 and Darco 12 × 40 were ground and sieved to 0.2 mm, while PAC200 was used directly. In the column tests, all the carbons were used as received. The surface characteristics of the carbons were determined in samples of pulverized carbon according to the methods detailed in the analytical methods section (see also Table 1).

Xylo-oligosaccharides were obtained by the autohydrolysis of grounded almond shells at 179 °C for 23 min. Full details of the reactor system and the operational procedure have been provided elsewhere.¹² Xylo-oligosaccharides from two different reaction batches were used in this study. The first batch comprised solid xylo-oligosaccharides recovered from the

autohydrolysis solution by spray drying. This procedure removed water and most of the volatile impurities such as furfural and acetic acid, leaving dry xylo-oligosaccharides (XOs) that still contained all the nonvolatile impurities, such as monosaccharides, organic extractives, lignin-derived phenolics, and inorganic salts. This sample was used for the adsorption equilibrium tests. The second batch comprised an XO solution prepared by autohydrolysis under the same conditions as the first but used directly for the continuous adsorption tests in packed columns. It had a total solids concentration of 35.2 g/L.

Adsorption on Activated Carbon. Adsorption equilibrium was measured in a batch system. A sample of the xylo-oligosaccharides of the first reaction batch recovered by spray drying was dissolved in deionized water at a concentration of 20 g/L. Aliquots of 10 mL of this solution were placed in 20 mL test tubes, and the appropriate amount of activated carbon was added (from 15 to 500 mg). The tubes were capped and placed in a water bath at 30 °C, attached perpendicularly with clamps to a horizontal revolving shaft that had a rotating speed of 2 rpm. After 24 h, the tubes were removed from the bath and the mixture was centrifuged at 4000 rpm for 20 min to precipitate the activated carbon. A sample of the supernatant liquid was filtered through a 0.22 μm nylon syringe filter, placed in an encapsulated HPLC vial, and stored at 5 °C until analysis.

Column tests were performed at room temperature (21 ± 1 °C) using around 22 g of granular activated carbon packed on a 55 mL column, with an inner diameter of 20 mm, made of metacrylate tube and PVC fittings. Activated carbon was submerged in boiling water for 15 min to remove air and fine particles and then extracted and poured immediately into the column, which had previously been filled with water to avoid entrapping air in the carbon bed. The column had wire mesh plates at both ends to prevent the entrainment of carbon particles and was operated in up-flow mode to reduce channeling. The solution of crude xylo-oligosaccharides from the second reaction batch was fed at 6 mL/min with a Watson-Marlow 313F peristaltic pump (Watson-Marlow Bredel, USA), which led to a residence time of 0.15 h. At the end of the experiment, the feed was switched to deionized water for 1 h to clean the column. The product was collected in four fractions—from 0 to 2 h (F1, 13.1 bed volumes circulating through the column), from 2 to 4 h (F2, 26.2 bed volumes), from 4 to 5.5 h (F3, 36 bed volumes), and the washing solution—and the dissolved solids in each fraction were recovered by lyophilization. Also, samples of 2 mL were withdrawn from the outlet stream throughout the experiment, filtered through a 0.22 μm nylon filter, and analyzed by gel permeation chromatography/high-performance liquid chromatography (GPC/HPLC) to determine the instantaneous composition of the product stream, as described below.

Analytical Methods. The surface area and porosity of the activated carbons were determined from their nitrogen adsorption-desorption isotherms obtained at 77 K in an ASAP 2020 surface analyzer (Micromeritics, USA). The samples were previously degassed at 523 K for several hours. N₂ adsorption data for P/P_0 from 10⁻⁵ to 0.99 were analyzed according to (i) the BET method²² for calculating the specific surface area, S_{BET} and (ii) the α_s method²³ using Carboxypack F Graphitized Carbon Black as reference material to calculate the ultramicropore volume²⁴ (pore diameter < 0.8 nm), $V_{\alpha, \text{mic}}$. The total pore volume, $V_{0.99}$, was calculated from nitrogen adsorption at a relative pressure of 0.99. The average pore diameter was calculated from the total pore volume and the surface area with eq 1. The point of zero charge (PZC) was determined by mass titration.²⁵ Various amounts of activated carbon were added to

2296 Ind. Eng. Chem. Res., Vol. 45, No. 7, 2006

a 10 mL solution of 0.1 M NaCl to obtain mixtures with 0.05, 0.1, 0.5, 1.0, and 10% of carbon by weight. The bottles were sealed to eliminate any contact with air and stirred overnight. The equilibrium pHs of the suspensions were measured after 24 h of contact time. The PZC value of the activated carbon was taken as the equilibrium pH of the suspension with the highest concentration of carbon when the change in pH with carbon concentration was low. Methylene blue ($C_{16}H_{18}ClN_3S \cdot 2H_2O$, MB) serves as a model compound for checking the adsorption of medium-size organic molecules from aqueous solutions. A 50 mL portion of a 3.2 mM solution of MB (Scharlau Chemie, Spain) and approximately 50 mg of activated carbon were used in adsorption experiments. The solutions were stirred overnight and filtered to remove the activated carbon in suspension before analysis. The equilibrium concentration of MB in the solution was measured by spectrometry at 664.8 nm in a Dinko Instruments 8500 spectrometer (Dinko Instruments, Spain). The amount adsorbed was calculated from the change in concentration of the solution. The iodine number was provided by NORIT. The oxygenated acid surface groups were determined according to the method of Boehm,²⁶ and the basic groups were determined by titration with hydrochloric acid. A 25 mg portion of carbon was mixed with 25 mL of each of the following solutions: 0.1 N sodium hydroxide, 0.1 N sodium carbonate, 0.1 N sodium bicarbonate, 0.1 N sodium ethoxide, and 0.05 N hydrochloric acid. The vials were sealed and stirred for 48 h, and the solutions were filtered. Samples of 5 mL were taken. These were titrated with 0.05 N HCl or 0.1 N NaOH to determine the excess of base or acid, respectively. The number of acidic sites of each type was calculated under the assumptions that sodium ethoxide neutralizes all the acidic groups (i.e., the carboxylic, phenolic, lactonic, and carbonyl groups), that NaOH neutralizes the carboxylic, phenolic, and lactonic groups, that Na_2CO_3 neutralizes the carboxylic and lactonic groups, and that $NaHCO_3$ neutralizes only the carboxylic groups. The number of surface basic sites was calculated from the amount of HCl consumed by the activated carbon.

$$\bar{d}_p = 4 \frac{V_{0.99}}{S_{BET}} \quad (1)$$

Solid xylo-oligosaccharides were analyzed for their ash content (ASTM D 1102-84 standard method) and for carbohydrates, acetyl groups, and lignin. A sample was dissolved in deionized water and analyzed (i) by HPLC to quantify the free monosaccharides (glucose, xylose, and arabinose), acetic acid, furfural, and hydroxymethyl furfural (HMF) and (ii) by HPLC/GPC to determine the molar mass distribution. Another sample of the XOs was dissolved in 4% sulfuric acid and was quantitatively hydrolyzed at 120 °C for 45 min to convert the oligosaccharides into their constitutive monomers. The hydrolyzate was analyzed by HPLC, and the amount of xylo-oligosaccharides was estimated from the monosaccharides and acetic acid liberated by the quantitative hydrolysis. Lignin was measured as the insoluble residue after the quantitative hydrolysis (Klason-type lignin) by the TAPPI UM 250 method for the acid-soluble lignin. The XO solution from the autohydrolysis reactor (2nd batch of XO) was analyzed with the same procedures. HPLC analyses were performed with a Bio-Rad HPX 87H column at 30 °C (Bio-Rad Laboratories, USA) in an Agilent 1100 series chromatograph (purchased from Agilent, Barcelona, Spain). The solvent was 0.005 M H_2SO_4 at a flow rate of 0.5 mL/min. An Agilent 1100-DAD ultraviolet (UV) diode-array detector and an Agilent 1100-RID refractive index (RI) detector were connected in series. The UV detector was

used to quantify furfural and HMF in the samples that contained low concentrations of these compounds. The RI detector was used for the samples with high concentrations of furfural and HMF and for carbohydrates. The molar mass distribution of the xylo-oligosaccharides was determined by GPC using the same chromatograph and the GPC add-on of the LC Chemstation software (purchased from Agilent, Barcelona, Spain). The analyses were performed with a TSK Gel G3000PWXL column (Toso Haas, purchased from Teknokroma, Barcelona, Spain) at 25 °C using 0.5 mL/min of a 0.05 mol/L solution of KNO_3 with 83 mg of sodium azide as solvent and the refractive index detector. The system was calibrated with xylose, glucose, and low-polydispersity standards of malto-oligosaccharides and dextrans (Fluka). In all cases, the samples were filtered through a 0.22 μm nylon syringe filter prior to HPLC analyses.

Results and Discussion

Adsorption Equilibrium Tests. Adsorption equilibrium tests were developed using a sample of crude xylo-oligosaccharides obtained by spray drying of the hydrolysis liquor (batch 1). This sample comprised 58.3% xylo-oligosaccharide, 5.0% monomer products (2.4% xylose, 1.5% arabinose, 0.78% glucose, 0.27% HMF, and trace amounts of acetic acid and furfural), 4.8% ash, and 16% Klason-type lignin. The remaining 14.9% of the solid was made up of compounds from the almond shells that were solubilized during the autohydrolysis reaction, e.g., extractives, low molar mass phenolics from lignin, and byproducts from the degradation and condensation of monosaccharides and furfural, which were not identified with the analytical procedures we used.

The adsorption of the carbohydrate and lignin-derived fractions of the xylo-oligosaccharides on activated carbons was tested at 30 °C using a constant concentration of crude xylo-oligosaccharides of 20 g/L in deionized water and concentrations of activated carbon of 1.5, 3.3, 10.0, 16.7, 30.0, and 50.0 g_A/g_C . Figure 1 shows the GPC chromatograms of the feed solution. The UV signal at 254 nm was attributed to the presence of compounds derived from lignin and extractives and from their condensation with furfural, HMF, and other carbohydrate-degradation products, which accounted for around 30% of the mass of the sample. We assumed that the signal of the refractive index detector was caused mainly by carbohydrates and inorganic salts (soluble ashes), since they constituted nearly 70% of the mass in the crude xylo-oligosaccharides, though all the species in the mixture contributed to the signal of this nonselective detector. The retention times for narrow standards of dextran, malto-oligosaccharides, and xylose are included in Figure 1 for comparison. The RI signal shows that the xylo-oligosaccharides had a molar mass below 50 kDa. The most abundant species had a molar mass of between 1 and 5 kDa. There was also a small fraction of the mixture with a molar mass of below 0.15 kDa (xylose). Some of this was inorganic salts (ashes) that eluted after monosaccharides in this chromatographic system. Data from the UV signal revealed two important facts. First, a significant amount of lignin-derived products eluted at the same interval of retention time as did the xylo-oligosaccharides. This was in agreement with the existence of phenolic side groups such as ferulic acids and lignin fragments, which are directly attached to the xylan backbone chains.²⁷ Second, almost half of the lignin-derived products were eluted at a retention time that was well above that of xylose (0.15 kDa). These products were low-molar mass phenolics that eluted from the chromatographic column with a different pattern from that of oligosaccharides, partly because they may have

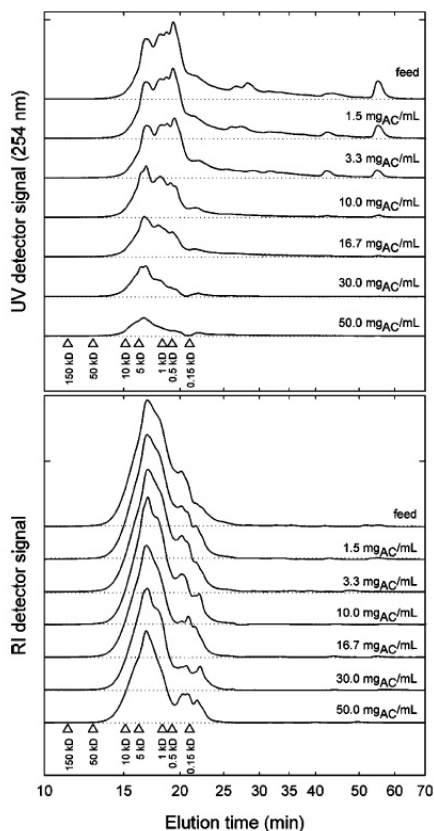


Figure 1. GPC chromatograms (time in log scale) for the xylo-oligosaccharides remaining in solution in the equilibrium adsorption experiments at 30 °C and different loads of the AC-1 activated carbon. The UV signal at 254 nm (top) is caused by lignin-derived phenolics, while the refractive index signal (bottom) is mainly attributed to carbohydrates (oligomers and monomers).

hydrodynamic volumes in 0.05 mol/L KNO_3 that are lower than those of carbohydrates of equivalent molar mass, but mainly because of adsorption on the gel of the GPC column, which increases the elution time. Palm and Zacchi²⁸ observed the adsorption of lignin-derived compounds from wood autohydrolysis on the gel of filtration columns.

Figure 1 also shows the GPC chromatograms for selected samples of the xylo-oligosaccharide solution treated with AC-1. The low molar mass lignin-derived products, which have the longest elution times in the GPC system, are preferentially adsorbed when small amounts of activated carbon are added to the solution. Figure 1 shows that they were completely adsorbed when 16.7 $\text{g}_{\text{AC}}/\text{L}$ was used. The lignin-products in the range of the elution time of oligosaccharides were also adsorbed, but they were still detected even at 50 $\text{g}_{\text{AC}}/\text{L}$ since they are linked to xylose in xylo-oligosaccharides. The adsorption of the carbohydrate fraction was less significant. Below a carbon load of 16.7 $\text{g}_{\text{AC}}/\text{L}$, only species with a molar mass of below 0.5 kDa were adsorbed. At a higher carbon load, there was a reduction in the signal of the sample at all molar masses, but even at 50 $\text{g}_{\text{AC}}/\text{L}$, the total amount of carbohydrates adsorbed was still below 40%. The same qualitative trends were observed for the other activated carbons we tested.

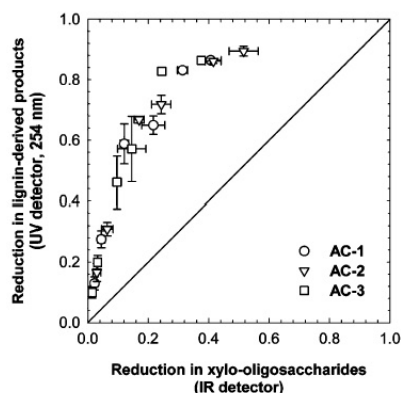


Figure 2. Relation between the reduction in the concentrations of lignin-derived phenolics and carbohydrates at equilibrium for various loads of activated carbon at 30 °C. Error bars are confidence intervals at the 95% probability level.

The reductions in the concentrations of lignin-derived products and carbohydrates (r_{d_j}) were calculated from the areas of the GPC chromatograms by assuming constant response factors (eq 2), and the amounts of each solute adsorbed were calculated from a mass balance for the batch system using eq 3, in which j indicates lignin-derived products or carbohydrates, $C_{0,j}$ (g/L) is the concentration of solute in the feed, $C_{e,j}$ (g/L) is the equilibrium concentration of species j in the solution, $C_{\text{Se},j}$ ($\text{g}/\text{g}_{\text{AC}}$) is the concentration of solute j adsorbed on the activated carbon at equilibrium, m is the mass of activated carbon (g_{AC}), and V is the volume of the solution (L). Figure 2 shows the reduction in the concentrations of lignin-derived products and xylo-oligosaccharides in solution for the three activated carbons we tested. Lignin-derived products were preferentially adsorbed over the carbohydrate fraction, especially at low concentrations of AC when the low molar mass aromatics were adsorbed. For instance, when 70% of the lignin-derived compounds were adsorbed, around 80% of the carbohydrates were still in solution. When over 80% of these compounds were adsorbed, the adsorption of carbohydrates dramatically increased.

The adsorption of mixtures of organic solutes onto activated carbons is a complex process that is determined by the chemistry of the carbon surface, the interactions between the solutes and the surface, the interactions of the solutes with the solvent, and those of the solvent with the carbon surface. The molar mass of the solute and the distribution of pore diameters of the carbon also play a significant role in determining the fraction of carbon surface that is actually accessible to a specific solute. The preferential adsorption of lignin-derived species over xylo-oligosaccharides may be attributed to several factors. Lignin-derived species are substituted phenolic monomers and oligomers that are more hydrophobic than carbohydrates. Xylo-oligosaccharides will therefore be more stable in water solution than lignin-derived products especially if, as in activated carbons, the surface of the adsorbent is predominantly hydrophobic.

Average pore diameters were 2.4, 2.1, and 4.1 nm for AC-1, AC-2, and AC-3, respectively. Table 2 shows that the activated carbons had a significant fraction of micropores, while Figure 3 shows that the pore volume distribution, which was calculated with the density functional theory (DFT) model,²⁹ was different for the three carbons. Most of the mesopore volume in the AC-1 carbon corresponded to pores with diameters from 2 to 10 nm, and the rest corresponded to large mesopores (30–50 nm). The

2298 Ind. Eng. Chem. Res., Vol. 45, No. 7, 2006

Table 2. Freundlich Isotherms: Results for the Adsorption of the Carbohydrate Fraction and the Lignin-Derived Products on Commercial Activated Carbons^a

	AC-1 (ROX 0.8)	AC-2 (PAC200)	AC-3 (Darco 12 × 40)
Xylo-oligosaccharides			
n	1.00 ± 0.13	0.81 ± 0.11	0.66 ± 0.09
$K_{XO}[L^{(1/n)} / (g_{ACG}^{(1/n)} - 1)]$	0.0148 ± 0.0046	0.0324 ± 0.0084	0.0249 ± 0.0054
Lignin-Derived Products			
n	0.82 ± 0.06	0.82 ± 0.05	0.62 ± 0.05
$K_{LP}[L^{(1/n)} / (g_{ACG}^{(1/n)} - 1)]$	0.145 ± 0.008	0.184 ± 0.009	0.134 ± 0.007

^a Confidence intervals were calculated at $\alpha = 0.05$.

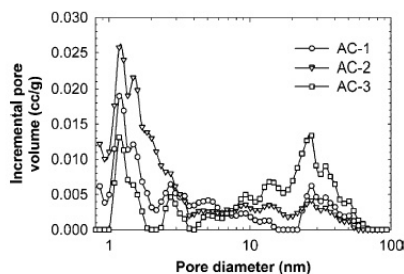


Figure 3. Pore volume distributions for the three activated carbons used in this study.

AC-2 carbon had the largest mesopore pore volume, but it had more pore volume than the AC-1 in the zone of small mesopores and a similar amount of large mesopores. Finally, the AC-3 carbon had very low volume in the small mesopore region, and most of its mesopore volume corresponded to large pores, from 10 to 50 nm. Around half of the lignin-derived compounds and associated impurities that are present in the crude xylo-oligosaccharides had a low molar mass (i.e., around 0.1 kDa) and were easily adsorbed in the three activated carbons, since their entire surface was accessible to these small solute molecules. On the other hand, xylo-oligosaccharides and some of the lignin-derived impurities had molar masses from 1 to 50 kDa, which is roughly equivalent to an interval of molecular diameters from 2 to 10 nm. The area available for the adsorption of the oligomers was therefore dependent on their molar mass: the larger the molar mass, the lower the area they could access. This effect should be more important for carbons AC-1 and AC-2, which have a significant fraction of pores below 10 nm.

However, solute size and the pore diameters are not the only variables governing adsorption. If we compare the GPC chromatograms in Figure 1 for xylo-oligosaccharides and lignin products at a high concentration of carbon AC-1, we can see that the reduction in the concentration of high molar mass solutes was much greater for the lignin products than for xylo-oligosaccharides. The presence of carboxylic and other acidic groups on the surface of the carbon has a definite effect on the adsorption of phenol, since it favors the chemisorption of phenol but hinders physisorption.³¹ We may expect the same to be true for the lignin-derived phenolics present in the crude xylo-oligosaccharides. Finally, electrostatic interactions between charged solutes and the surface of the carbon must also be considered. The pH of the xylo-oligosaccharide solution was 5.7 due to the dissociation of the acetyl groups in the backbone chain of the xylo-oligosaccharides and the carboxyl groups in ferulic acids and in some lignin-derived products. Since this pH is below the pH of zero charge of the activated carbons ($8 < \text{pH}_{\text{PZC}} < 8.7$), we can expect the surface of the carbons to have a positive charge distributed among the basic superficial groups.³¹ This should create favorable electrostatic interactions

between the positive surface and the negatively charged solutes such as the xylo-oligosaccharide chains that contain dissociated acetyl groups.

$$rd_j = 1 - \frac{C_{e,j}}{C_{0,j}} \quad (2)$$

$$C_{Se,j} = \frac{V}{m}(C_{0,j} - C_{e,j}) \quad (3)$$

$$\ln C_{Se,j} = \ln K_j + n_j \ln C_{e,j} \quad (4)$$

Regardless of the complexity of the phenomena involved in the competitive adsorption of mixtures of polydisperse oligomers with dissimilar chemical structures, simple models can provide some insight into the factors that have a determining influence on the selective adsorption of lignin-related species over xylo-oligosaccharides. Adsorption equilibrium was modeled through the Freundlich isotherm, which relates the concentration of a j solute at equilibrium ($C_{e,j}$) to the concentration of j adsorbed on the surface ($C_{Se,j}$). The unit-capacity parameter, K_j , is a measure of the degree of strength of adsorption, and n_j , the site-energy parameter, is an indication of the heterogeneity of the surface adsorption sites. The closer the value of n_j is to unity, the more homogeneous is the energy of the surface sites. The Freundlich isotherm was linearized to calculate the constants n_j and K_j (eq 4). Figure 4 shows the linearized isotherms, and Table 2 shows the best-fit values of n_j and K_j for the three activated carbons and their confidence intervals at 95% probability. Calculations were done using the robust linear regression algorithm implemented in the *robustfit* function of the statistics toolbox of MATLAB (MathWorks Inc., USA). The isotherm provided an acceptable description of the adsorption of both the lignin-derived products and carbohydrates for the three activated carbons, since the model predictions fell within the scattering of the experimental data.

Possible correlations between the main properties of the activated carbons and the parameters of the Freundlich equation for xylo-oligosaccharides and lignin-derived products were analyzed. Figure 5 shows that the unit-capacity parameter for xylo-oligosaccharide adsorption (K_{XO}) increased with the mesopore volume of the activated carbon, while the site-energy parameter increased linearly with the concentration of basic surface groups. The carbons with more developed mesoporous structures had more surface area available for the adsorption of xylo-oligosaccharides with larger molar mass, thus giving higher values for the unit-capacity parameter of the Freundlich isotherm. Also, the higher the number of basic surface groups on the surface, the stronger the electrostatic interactions between the dissociated acetyl groups of the xylo-oligosaccharide chains and the positively charged surface, thus increasing the site-energy parameter n_{XO} for xylo-oligosaccharides adsorption. The K_{LP} parameter for the lignin-derived phenolics grew with the total concentration of acidic superficial groups. In studies on

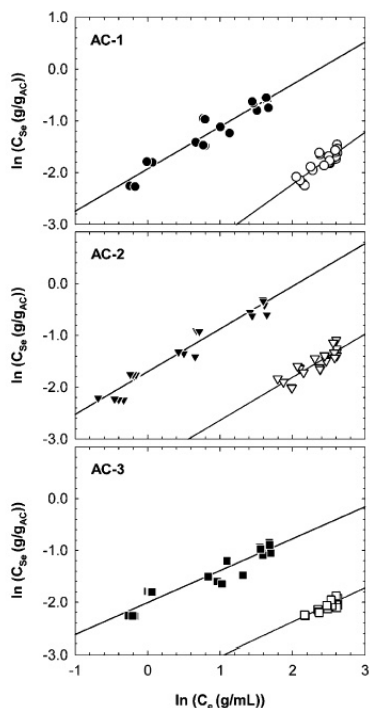


Figure 4. Freundlich isotherms for the adsorption of lignin-derived phenolics (open symbols) and xylo-oligosaccharides (solid symbols) on the three activated carbons at 30 °C.

phenol adsorption from acidic water solutions, the increase in the unit-capacity parameter with the concentration of acidic surface groups has been explained by the existence of two parallel routes: physical adsorption and acid-catalyzed chemisorption.³⁰ We may expect the contribution of chemisorption to the overall adsorption of the low molar mass phenolics present

in the complex mixture of lignin-related products to become more important as the number of acidic surface groups increases, thus increasing K_{LP} . In contrast, the site-energy parameter, n_{LP} , did not have a clear correlation with the concentration of acidic surface groups. Promoting the surface acidic groups by oxidation of an activated carbon reduces the adsorption of phenol from aqueous solution.³¹ More acidic groups should favor chemisorption, but they lower physical adsorption because the acidic groups act as electron acceptors and lower the π -electron density in the carbon planes, thus decreasing the interaction between the aromatic rings and the carbon basal planes. Since physical adsorption is the dominant mechanism, the overall consequence is lower phenol adsorption and a decrease in the site-energy parameter, n , of the Freundlich isotherm.³⁰ In our case, it seems that n_{LP} increased for activated carbons with more acidic surface groups, though the values of n_{LP} for AC-1 (0.82 ± 0.06) and AC-2 (0.82 ± 0.05) were statistically the same even if they had different concentrations of acidic surface groups (6.0 mequiv/g for AC-1 and 7.9 mequiv/g for AC-2). This behavior may be caused by the different nature of the predominant acidic groups in each carbon, which were manufactured from a variety of raw materials using different methods of activation. Phenols are the main acidic group in AC-1 (4.2 mequiv/g), while in AC-2 the main group is carbonyls (4.6 mequiv/g). The relative importance of the chemisorption and physical adsorption paths will therefore be different in each carbon due to the different acidity of these groups. Finally, no direct correlations of the Freundlich parameters with other properties of the activated carbons such as the surface area or the total pore volume were observed.

On the basis of the analysis of the Freundlich isotherms, the purification of xylo-oligosaccharides will require activated carbons with unit-capacity and site-energy parameters that are low for xylo-oligosaccharides and high for lignin-derived products. The AC-1 carbon, with a K_{LP}/K_{XO} of 9.8 ± 3.6 , had a slightly better ratio of unit-capacities than AC-2 (5.7 ± 1.8) and AC-3 (5.4 ± 1.4), while the ratio n_{LP}/n_{XO} did not present significant differences due to the large scattering of the results (0.82 ± 0.17 for AC-1, 1.01 ± 0.20 for AC-2, and 0.94 ± 0.20

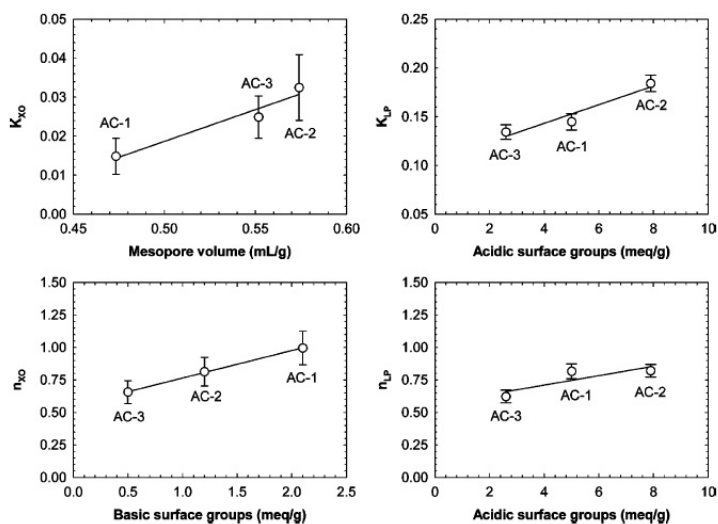


Figure 5. Variation in the constants of the Freundlich isotherms of lignin-derived compounds and xylo-oligosaccharides (K_{LP}) with the surface properties of the activated carbons. The lines only indicate trends.

2300 Ind. Eng. Chem. Res., Vol. 45, No. 7, 2006

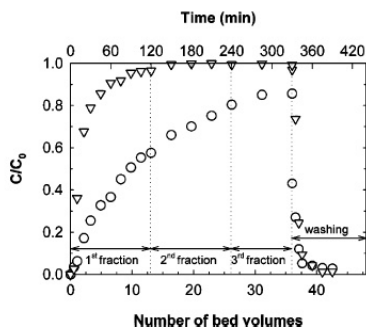


Figure 6. Adsorption of the crude xylo-oligosaccharides from reaction batch 2 on an AC-1 activated carbon column: breakthrough curves for carbohydrates (∇) and lignin-derived products (\circ).

for AC-3). In general, a suitable activated carbon should have small mesopore diameters, a low volume of mesopores, and a low concentration of basic surface groups to limit xylo-oligosaccharide adsorption. It should also be highly microporous and have acidic surface groups to favor the adsorption of the lignin-related products (high K_{LP}).

Column Tests. Column tests were performed with the ROX 0.8 granular activated carbon (AC-1). This carbon was selected because of its slightly better selectivity toward lignin adsorption and because it was readily available in granular form and more suitable for column packing than AC-2 and AC-3. The latter contained fines and caused problems during operation due to the entrainment of carbon particles and because it led to larger pressure drops across the bed. Figure 6 shows the breakthrough curves for an experiment performed using the second batch of xylo-oligosaccharides solution directly. The solution was fed at 6.0 mL/min, and a column loaded with 22.0 g of activated carbon was used. The activated carbon was rapidly saturated with carbohydrates. Retention for carbohydrates was only 10% after 60 min (6.55 bed volumes circulated), while retention for lignin-derived products was over 60%. After 180 min (19.6 bed volumes), the column was completely saturated with carbohydrates and retention was 0.2% but it was still 30% for lignin products. Figure 7 shows the GPC chromatograms for samples of the effluent taken at selected times during the experiment. The lignin-derived products of low molar mass were completely adsorbed on the column during the first 45 min of the experiment, which corresponds to 4.91 bed volumes of feed circulated through the column, but the high molar mass fraction of lignin products associated to carbohydrates was not adsorbed completely even when the volume circulated was small (2.18 bed volumes). The carbohydrate fraction had low adsorption, and there were few differences in the degree of adsorption with molar mass. The fraction collected during the cleaning of the carbon bed with deionized water contained both carbohydrates and lignin-derived species. The latter were detected in the washing stream even after 60 min of cleaning (6.55 bed volumes of water), which suggests that they were strongly adsorbed on the surface of the carbon.

The fractions collected during the experiment were lyophilized to recover the xylo-oligosaccharides (F1, 0–2 h; F2, 2–4 h; F3, 4–5.5 h; F4, washing, 5.5–6.5 h). The dry product was weighed to calculate the yield and analyzed for ash, klason lignin, monomers, xylo-oligosaccharides, and the molar mass distribution. Table 3 shows that the average concentration of nonvolatile soluble products decreased from 35.2 g/L in the feed to 25.2 g/L in the product collected from the column outlet

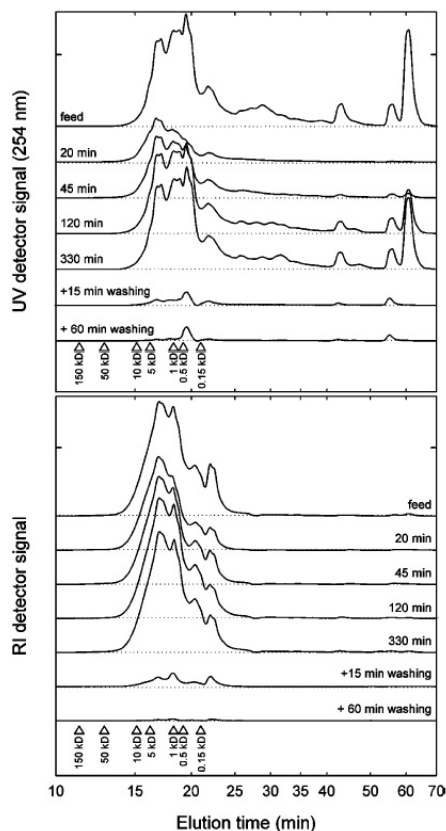


Figure 7. Adsorption of the crude xylo-oligosaccharides from reaction batch 2 on an AC-1 activated carbon column: GPC chromatograms (time in log scale) for the xylo-oligosaccharides remaining in solution. The UV signal at 254 nm (top) is caused by lignin-derived phenolics, while the RI signal (bottom) is mainly attributed to carbohydrates (xylo-oligosaccharides and monomers).

during the first 2 h of the experiment. Analysis of the recovered product shows that monosaccharides and xylo-oligomers were partially adsorbed on the carbon, but the highest adsorption was for lignin-related products and for furfural and HMF, which were almost completely removed from the solution. The product fractions collected afterward (F2 and F3) showed a dramatic decrease in the capacity of adsorption of the column for carbohydrates, although some retention capacity was still observed for furfural, HMF, and lignin-derived species.

The retention for carbohydrates, mainly xylo-oligosaccharides but also monosaccharides, was calculated by integrating the RI signal of the GPC chromatograms of the feed and the samples taken during the experiment, whereas the retention for lignin and carbohydrate-degradation products (furfural and HMF) was calculated from the signal of the UV detector at 254 nm. Retentions for fractions F1–F3 were 20.2, 0.7, and 0.5% for carbohydrates and 64.3, 30.2, and 16.0% for lignin, in accordance with the preferential adsorption of lignin products over carbohydrates we observed earlier. The retentions were also calculated from the mass and composition of the nonvolatile products recovered by lyophilization of the fractions F1, F2, and F3. The results were close to those calculated from the GPC chromatograms, especially for carbohydrates.

Table 3. Adsorption on an AC-I Activated Carbon Column: Composition of the Lyophilized Samples of the Product Fractions Collected during the Experiment and Retentions Calculated for Xylo-oligosaccharides and Lignin-Related Products (Xylo-oligosaccharide Solution from Reaction Batch 2)

	feed	collected fractions		
		F1 (0–2 h)	F2 (2–4 h)	F3 (4–5.5 h)
avg conc of dissolved products for the fraction (g/L)	35.2	25.2	33.6	33.9
Composition (% of the Dissolved Products in the Feed)				
glucose	1.84	1.28	1.76	1.75
xylose	3.95	2.81	3.96	3.97
arabinose	3.61	2.58	3.58	3.57
acetic acid	3.89	1.74	3.78	3.85
furfural	0.85	0.01	0.40	0.87
hydroxymethyl furfural	0.43	0.03	0.26	0.39
xylo-oligosaccharides	57.8	46.0	59.3	58.6
lignin-related products	6.85	2.90	5.55	5.95
ash	9.02	7.66	7.36	7.60
other (by difference)	11.8	6.78	9.49	9.84
Retention (% of Feed)				
xylo-oligosaccharides (RI signal)	calculated by integration of the GPC chromatograms (data in Figure 7)			
		20.2	0.7	0.5
lignin-related products (UV signal)	calculated from the yield and chemical analysis of lyophilized samples			
		64.3	30.2	16.0
xylo-oligosaccharides ^a		22.5	0.5	0.9
lignin-related products ^b		63.9	23.6	11.4

^a Including monosaccharides, acetic acid, and ash. ^b Including furfural and HMF.

Vegas and co-workers have investigated several sequential treatments for the removal of extractive- and lignin-derived compounds from the aqueous solutions of crude xylo-oligosaccharides of barley residues¹³ and rice husks.¹⁴ After three sequential extraction stages with ethyl acetate, 6.2% of the carbohydrates and 38.2% of non-carbohydrates were removed from the solution in the case of rice husks, while for barley residues removal was 15.9% for carbohydrates and 32.9% for extractives- and lignin-related products. These values are close to those we obtained for fraction F2. Further processing of the ethyl acetate-extracted solutions with a strong anion-exchange resin increased the removal of non-carbohydrates to 78.2 and 54.0% for rice husks and barley residues, respectively, while carbohydrate removal was 22.2 and 20.4%. Our results from the F1 fraction indicate that treatment with activated carbon provides better results than extraction with ethyl acetate and that it may even produce a similar degree of removal of non-carbohydrate compounds to extraction combined with treatment with anion-exchange resins.

Conclusions

The treatment with activated carbon of raw xylo-oligosaccharide solutions obtained by autohydrolysis of lignocellulosics is a feasible option for the removal of extractives- and lignin-derived compounds and carbohydrate-degradation products. The selective adsorption of lignin products over carbohydrates has been observed for three commercial activated carbons at slightly acidic pHs. Selectivity toward lignin adsorption was higher when the carbon was highly microporous and had small mesopore diameters, a low volume of mesopores, a low concentration of basic surface groups to limit xylo-oligosaccharide adsorption, and acidic surface groups to favor the adsorption of the lignin-related products. Further studies into the tailoring of the surface properties of the carbons in order to improve selectivity and adsorption capacity for lignin-products, and into the regeneration of spent carbon beds, are under way.

Acknowledgment

This research was made possible in part by financial support from the Spanish Government (MCYT, project PPQ2002-04201-CO02), the Catalan Regional Government (DURSI,

2001SGR00323 and 2002AIRE), and the ALFA Program of the EU (project ALFA II 0412 FA FI). V.F. acknowledges the MCYT and the Universitat Rovira i Virgili (URV) for the financial support of her "Ramón y Cajal" research contract. D.N. is grateful to the Catalan Regional Government for her Ph.D. scholarship. V.T. is grateful to the URV for her Ph.D. grant, and A.M. is grateful to the Spanish Ministry of Education for economic support. The authors thank the NORIT Company for supplying the samples of their activated carbons.

Literature Cited

- Hudson, M. J.; Marsh, P. D. Carbohydrate metabolism in the colon. In *Human colonic bacteria - role in nutrition, physiology and pathology*; Gibson, G. R., MacFarlane, G. T., Eds.; CRC Press: Boca Raton, FL, 1995; pp 61–73.
- Fooks, L. J.; Gibson, G. R. In vitro investigations of the effect of probiotics and prebiotics on selected human intestinal pathogens. *FEMS Microbiol. Ecol.* **2002**, *39*, 67–75.
- Fooks, L. J.; Gibson, G. R. Mixed culture fermentation studies on the effects of synbiotics on the human intestinal pathogens *Campylobacter jejuni* and *Escherichia coli*. *Anaerobe* **2003**, *9*, 231–242.
- Zampa, A.; Silvi, S.; Fabiani, R.; Morozzi, G.; Orpianesi, C.; Cresci A. Effects of different digestible carbohydrates on bile acid metabolism and SCFA production by human gut micro-flora grown in an in vitro semi-continuous culture. *Anaerobe* **2004**, *10*, 19–26.
- Crittenden, R.; Playne, M. Production, properties and applications of food-grade oligosaccharides. *Trends Food Sci. Technol.* **1996**, *7*, 353–361.
- Kontula, P.; von Wright, A.; Mattila-Sandholm, T. Oat bran β -gluco and xylo-oligosaccharides as fermentative substrates for lactic acid bacteria. *Int. J. Food Microbiol.* **1998**, *45*, 163–169.
- Glasser, W. G.; Jain, R. K.; Sjøstedt, M. A. Thermoplastic pentosan-rich polysaccharides from biomass. U.S. Patent 5,430,142, 1995.
- Gabrieli, I.; Gatenholm, P.; Glasser, W. G.; Jain, R. K.; Kenne, L. Separation, characterization and hydrogel-formation of hemicellulose from aspen wood. *Carbohydr. Polym.* **2000**, *43*, 367–374.
- Ando, H.; Ohba, H.; Sakaki, T.; Takamine, K.; Kamino, Y.; Moriwaki, S.; Bakalova, R.; Uemura, Y.; Hatate, Y. Hot-compressed-water decomposed products from bamboo manifest a selective cytotoxicity against acute lymphoblastic leukemia cells. *Toxicol. in Vitro* **2004**, *18*, 765–771.
- Korte, H. E.; Offermann, W.; Puls, J. Characterization and preparation of substituted xylo-oligosaccharides from steamed birchwood. *Holzforschung* **1991**, *45*, 419–424.
- Puls, J.; Schuseil, J. Chemistry of hemicelluloses: relationship between hemicellulose structure and enzymes required for hydrolysis. In *Hemicellulose and Hemicellulases*; Coughlan, M. P., Hazlewood, G. P., Eds.; Portland Press: London, 1993; pp 1–27.

2302 Ind. Eng. Chem. Res., Vol. 45, No. 7, 2006

- (12) Nabarlaz, D.; Fariol, X.; Montané, D. Autohydrolysis of almond shells for the production of xylo-oligosaccharides: product characteristics and reaction kinetics. *Ind. Eng. Chem. Res.* **2005**, *44*, 7746–7755.
- (13) Vegas, R.; Alonso, J. L.; Domínguez, H.; Parajó, J. C. Manufacture and refining of oligosaccharides from industrial solid wastes. *Ind. Eng. Chem. Res.* **2005**, *44*, 614–620.
- (14) Vegas, R.; Alonso, J. L.; Domínguez, H.; Parajó, J. C. Processing of rice husk autohydrolysis liquors for obtaining food ingredients. *J. Agric. Food Chem.* **2004**, *52*, 7311–7317.
- (15) Parajó, J. C.; Domínguez, H.; Domínguez, J. M. Study of charcoal adsorption for improving the production of xylitol from wood hydrolysates. *Bioprocess Eng.* **1995**, *16*, 39–43.
- (16) Gurgel, P. V.; Mancilla, I. M.; Peçanha, R. P.; Siquiera, J. F. M. Xylitol recovery from fermented sugarcane bagasse hydrolyzate. *Bioresour. Technol.* **1995**, *52*, 219–223.
- (17) Couteau, D.; Mathaly, P. Purification of ferulic acid by adsorption after enzymatic release from sugar-beet pulp extract. *Ind. Crops Prod.* **1997**, *6*, 237–252.
- (18) Couteau, D.; Mathaly, P. Fixed-bed purification of ferulic acid from sugar-beet pulp using activated carbon: optimization studies. *Bioresour. Technol.* **1998**, *60*, 17–25.
- (19) Lee, J. W.; Kwon, T. O.; Moon, I. S. Adsorption of monosaccharides, disaccharides, and maltooligosaccharides on activated carbon for separation of maltopentaose. *Carbon* **2004**, *42*, 371–380.
- (20) Ahmedna, M.; Marshall, W. E.; Rao, R. M. Surface properties of granular activated carbons from agricultural byproducts and their effects on raw sugar decolorization. *Bioresour. Technol.* **2000**, *71*, 103–112.
- (21) Yuan, Q. P.; Zhang, H.; Qian, Z. M.; Yang, X. J. Pilot-plant production of xylo-oligosaccharides from corn cob by steaming, enzymatic hydrolysis and nanofiltration. *J. Chem. Technol. Biotechnol.* **2004**, *79*, 1073–1079.
- (22) Brunauer, S.; Emmett, P. H.; Teller, E. Adsorption of Gases in Multimolecular Layers. *J. Am. Chem. Soc.* **1938**, *60*, 309–319.
- (23) Sing, K. S. W. The use of physisorption for the characterization of microporous carbons. *Carbon* **1989**, *27*, 5–11.
- (24) Kruk, M.; Li, Z. J.; Jaroniec, M.; Betz, W. R. Nitrogen Adsorption Study of Surface Properties of Graphitized Carbon Blacks. *Langmuir* **1999**, *15*, 1435–1441.
- (25) Noh, J. S.; Schwarz, J. A. Effect of HNO₃ treatment on the surface acidity of activated carbons. *Carbon* **1990**, *28*, 675–682.
- (26) Boehm, H. P. Chemical identification of surface groups. *Adv. Catal.* **1966**, *1*, 179–287.
- (27) De Vries, R. P.; Visser, J. *Aspergillus* enzymes involved in degradation of plant cell wall polysaccharides. *Microbiol. Mol. Biol. Rev.* **2001**, *65*, 497–522.
- (28) Palm, M.; Zacchi, G. Separation of hemicellulosic oligomers from steam-treated spruce wood using gel filtration. *Sep. Purif. Technol.* **2004**, *36*, 191–201.
- (29) Olivier, J. P. Improving the models used for calculating the size distribution of micropore volume of activated carbons from adsorption data. *Carbon* **1998**, *36*, 1469–1472.
- (30) Salame, I. I.; Bandosz, T. J. Role of surface chemistry in adsorption of phenol on activated carbons. *J. Colloid Interface Sci.* **2003**, *264*, 307–312.
- (31) Moreno-Castilla, C. Adsorption of organic molecules from aqueous solutions on carbon materials. *Carbon* **2004**, *42*, 83–94.

Received for review September 19, 2005
Revised manuscript received February 1, 2006
Accepted February 6, 2006

IE051051D

6. CONCLUSIONES GENERALES

La preparación de CA a partir de diferentes tipos de agentes activantes ácidos (H_3PO_4) o básicos (NaOH y KOH) a partir de lignina Kraft como material precursor, da como resultado carbones microporosos con altas áreas superficiales, con rendimientos a carbón razonables y con buenas propiedades para ser utilizados en la descontaminación de efluentes líquidos o gaseosos.

Conocer el efecto que la variación de las condiciones de operación produce es muy importante para poder controlar las características finales del producto, que depende de la aplicación que se le quiera dar. Para ello, es importante conocer el mecanismo de activación química que tiene lugar. En el caso de la activación con ácido fosfórico y a partir de datos experimentales, se han explicado los procesos reactivos que tienen lugar durante la pirólisis mediante una serie de reacciones de pseudoprimer orden, como resultado de

la simplificación de los múltiples procesos reactivos involucrados en la descomposición térmica que se ajusta correctamente a los escasos datos bibliográficos obtenidos.

El mecanismo de reacción que se propone se compone de dos etapas. En primer lugar, la mezcla entre la lignina y el ácido fosfórico dan lugar a un complejo generado por la reacción entre el ácido y los sitios reactivos de la lignina que puede durar aproximadamente una hora a temperatura ambiente y que se finaliza antes de comenzar el proceso térmico.

Posteriormente y una vez se comienza con la pirólisis de la muestra, se produce la conversión del exceso de ácido en P_2O_5 después de haberse eliminado por completo el agua presente en la mezcla. La formación de este compuesto está involucrada con el desarrollo de la estructura interna de la muestra ya que actúa como protección de la estructura y cuando seguidamente se evapora y produce la combustión de la muestra. Finalmente, la pirólisis completa del complejo generado en el primer paso, da lugar al CA definitivo y volátiles con lo que se acaba de desarrollar la estructura interna del producto final.

Una vez determinado los fenómenos que se producen en la activación química, es necesario conocer como afectan las condiciones de operación a las propiedades finales del carbón.

En el caso de la activación con H_3PO_4 , los parámetros estudiados son tres: el tiempo de impregnación, la temperatura de activación y la cantidad de ácido empleado.

Por un lado, la reacción de impregnación se completa en una hora y tiempos mayores no tienen ninguna influencia en la producción de carbón, al igual que la realización de isoterms localizadas durante el proceso pirolítico.

Respecto a la relación entre la cantidad de ácido fosfórico añadido y la de lignina Kraft, existe un máximo en el cual se produce la reacción completa de la lignina, situado en valores entre 0.8 y 1.0, y es a partir de este valor, no se producen cambios en el proceso de pirólisis que afecten a sus propiedades más importantes. A relaciones mayores de 1.4 comienza a disminuir el área superficial BET y el volumen total de poros promovido por el agresivo ataque del ácido fosfórico. El uso de ácido fosfórico en exceso produce óxidos de fósforo que protegen la estructura del carbón de la oxidación externa y cuando esta especie se evapora a temperaturas mayores de $580^\circ C$, el carbón se oxida totalmente en aire mientras que en presencia de nitrógeno, la producción de carbón se mantiene constante.

Por último, el aumento de la temperatura de activación de 400°C a 600°C produce un decremento en el volumen de ultramicroporos pero un aumento de la microporosidad total y es a esta temperatura, 600°C, donde se encuentra un óptimo para el desarrollo de la porosidad en este tipo de procesos. A partir de este punto, seguir aumentando la temperatura conlleva la reducción del volumen total de poros y de área superficial BET debido al colapso y al exceso de oxidación del material.

Por tanto, excepto el tiempo de impregnación, el resto de parámetros tienen una importante influencia en las características finales del CA. La disminución de superficie BET viene acompañada de un descenso considerable del rendimiento a carbón y se puede concluir que el valor óptimo respecto al desarrollo de la porosidad a una temperatura de 450°C está entre 1.2 y 1.4. El efecto del tiempo de impregnación es menos importante aunque su aumento provoca una ligera disminución del área superficial y del volumen total de poros. Este efecto tiene más importancia cuando se utilizan también altas temperaturas debido a la descomposición de los enlaces entre el carbón y los fosfatos y polifosfatos.

A parte de las condiciones de operación, otro factor que puede afectar a las condiciones finales del CA es la cantidad de cenizas que contiene la lignina Kraft, tal y como se suministra, en comparación con su uso una vez desmineralizada, es decir, después de proceder a un pretratamiento ácido.

Los análisis realizados por SEM y por espectroscopía de infrarrojo demuestran que el proceso de desmineralización de la materia prima produce un aumento en la polimerización de la lignina y reduce la interacción entre ésta y el ácido fosfórico. De esta manera, se ven afectadas las propiedades finales del AC-P de tal forma que al aumentar la temperatura de pirólisis, aumenta el rendimiento a carbón, la aromaticidad, el área superficial y la cantidad de grupos superficiales en los CA preparados a partir de LK, mientras que la tendencia es opuesta para los CA preparados a partir de LK_d.

En el caso de la activación química con NaOH y KOH, el uso de hidróxidos alcalinos en este tipo de procesos está desarrollando un incremento de interés, por esta razón la posibilidad de preparar CA microporosos a partir de lignina Kraft desmineralizada y KOH o NaOH es parte fundamental de esta memoria.

En este caso, las condiciones de operación estudiadas son cinco: la temperatura de activación, la relación entre agente activante y precursor, el

tiempo de impregnación, el flujo de nitrógeno empleado como atmósfera dinámica en el proceso y por último, la velocidad de calentamiento.

La temperatura de activación es uno de los parámetros que más influencia tiene en este tipo de activaciones. A medida que ésta aumenta y esencialmente a partir de 750°C, los carbones pasan de ser esencialmente microporosos a aumentar la cantidad de mesoporos, ya que a altas temperaturas se produce el colapso de la estructura interna provocando la transformación de los poros más pequeños en poros mayores. A partir de 700°C, se produce un desarrollo pronunciado de la química de superficie. En el caso de la acidez, este aumento viene dado por la presencia de fenoles, alcoholes y carbonilos, aunque depende del tipo de hidróxido empleado como agente activante.

La relación de la cantidad añadida de agente activante y lignina Kraft tiene un efecto muy marcado en la producción de carbón y en el área superficial BET. El aumento de este parámetro, disminuye el rendimiento a carbón obtenido ya que la reacción de activación se ve favorecida y por tanto, se generan más volátiles que a su vez desarrollan la estructura interna. El aumento de hidróxido incrementa el contenido de especies oxigenadas en la superficie del carbón favoreciendo su oxidación y desarrollando tanto la acidez superficial, fundamentalmente mediante fenoles, alcoholes y carbonilos, como la basicidad superficial.

El tiempo de activación no tiene una influencia destacable, ya que principalmente favorece la descomposición de sales superficiales dando lugar a óxidos de carbono que colaboran al desarrollo de la estructura interna de los este tipo de AC. En este caso, no hay un efecto claramente definido sobre el desarrollo de la química superficial ya que si es cierto que se produce un aumento general de la basicidad, el desarrollo de la acidez depende del agente activante utilizado. El uso de hidróxido de potasio favorece el desarrollo de la acidez mediante fenoles y lactonas pero si se utiliza hidróxido de sodio, la acidez disminuye.

El caudal de nitrógeno empleado no es un factor importante en la activación con hidróxidos. Su función principal es la de facilitar la eliminación de los volátiles que se generan durante el proceso térmico aunque si se aumenta de manera pronunciada, y a temperaturas bajas, provoca también la eliminación de agente activante (hidróxido y otras especies como óxidos de carbono y agua) disminuyendo ligeramente la activación. La química de superficie se ve afectada de igual manera, produciendo variaciones poco significativas de la acidez y la basicidad superficial.

Respecto a la velocidad de calentamiento, su aumento produce disminuciones en el área superficial ya que durante el proceso de activación térmica, el hidróxido se funde y la superficie específica aumenta, el tiempo de contacto con el carbón es menor y disminuye la activación producida.

En general, los factores que influyen en mayor manera en los parámetros de estudio son la temperatura de activación y la relación de la cantidad entre agente activante y lignina Kraft que maximizan el área BET hasta $3000\text{m}^2/\text{g}$ aproximadamente, con un volumen de microporos de $1.5\text{ cm}^3/\text{g}$, a 700°C y una R de 3.

Finalmente, una vez se tienen caracterizados los CA preparados por diferentes métodos, estos se pueden aplicar en el campo más adecuado. Una de las principales aplicaciones de estos carbones está en la adsorción de contaminantes, como metales pesados o componentes orgánicos en sistemas líquidos.

En este campo, los carbones preparados a partir de la activación química con ácido fosfórico, también poseen una desarrollada acidez superficial, característica que combinada con su buena PSD, asegura una adsorción favorable de iones metálicos en solución. La temperatura de carbonización es el factor que afecta de manera más significativa ya que, como se ha visto anteriormente, cambia la porosidad del material y degrada la acidez superficial. Las condiciones de preparación del AC-P más adecuadas para maximizar la adsorción de cobre (65 mg Cu/g) son de 500°C de temperatura y una P/L de 1.4.

Optimizar la producción de AC-Na para maximizar su capacidad de adsorción de componentes orgánicos es posible mediante técnicas estadísticas para el diseño de experimentos. La técnica seleccionada fue la Metodología de Respuesta de Superficie debido a que agrupa técnicas tanto matemáticas como estadísticas que resulta de gran ayuda cuando se analizan sistemas donde hay una variable respuesta, la adsorción de azul de metileno, que se ve afectada por varias variables. Como resultado, se obtuvo un carbón activado que adsorbe más azul de metileno que los carbones comerciales utilizados para comparar a unas condiciones de 783°C , un contenido de lignina Kraft desmineralizada en la mezcla inicial del 26.4 %, empleando $200\text{ cm}^3\text{ N}_2/\text{min}$. A estas condiciones, la capacidad de adsorción obtenida fue de 940 mg AM/g CA , la cual se correlaciona con el volumen de microporos de las muestras analizadas y, en menor manera, con la química de superficie, influencia que depende de la naturaleza ácida o básica del compuesto orgánico empleado.

Para el estudio de la eliminación de componentes orgánicos en efluentes líquidos, fenol y benceno, la química de adsorción obedece a una reacción de pseudo segundo orden la cual es más favorable para el fenol que para el benceno. Los CA que se han empleado como adsorbatos en estos análisis son tres carbones derivados de la lignina Kraft y activados con los tres agentes activantes presentados en este estudio, NaOH, KOH y H₃PO₄. No se puede determinar que modelo de adsorción, Freundlich, Langmuir o Tempkin, describe mejor el proceso físico que tiene lugar ya que los tres proporcionan buenos ajustes. Las capacidades de adsorción máximas que se alcanzan han sido de 170 mg fenol/g y 20 mg benceno/g para el carbón activado con NaOH, 165 mg fenol/g y 20 mg benceno/g para el carbón activado con KOH y 60 mg fenol/g y 8 mg benceno/g para el carbón activado con H₃PO₄.

Sin embargo, estos carbones pueden tener otro campo de aplicación como es el de aditivo en membranas o la purificación de oligosacáridos. Así, el AC-P también se ha utilizado para obtener membranas poliméricas compuestas, etapa previa a la obtención de reactores de membranas enzimáticos, utilizando el carbón inmovilizado en la matriz polimérica para adsorber enzimas directamente, o a través de un metal, cobre en este caso, gracias a su buena capacidad de adsorción. A pesar que existen muchos ámbitos de aplicación para este tipo de membranas, en este caso particular, se han utilizado para obtener y separar azúcares de muy bajo peso molecular (cerca del monómero) a partir de azúcares de tamaño superior.

El uso de AC-P en las membranas permite buenas capacidades de separación cumpliendo con el objetivo especificado, y a pesar de que localmente se obtuvo mejor adsorción de enzima con el uso del metal, no se pudo concluir que en general, la utilización de éste implicara mejores resultados. En este sentido, son necesarios más experimentos.

Por último, el uso de carbones comerciales en el tratamiento de xilo-oligosacáridos obtenidos a partir de la autohidrólisis de materiales procedentes de biomasa es factible ya que permite eliminar componentes derivados de la lignina y extractivos. Este proceso debe llevarse a cabo mediante adsorbatos con pH ácido y de gran superficie específica, es decir, muy microporosos y con mesoporosidad poco desarrollada. Las características del carbón necesario para llevar a cabo este tipo de operaciones se adecuan a los carbones obtenidos para la realización de esta tesis. Por tanto, en los siguientes pasos a seguir en este campo de investigación parecen adecuados el uso de AC-P, AC-K y AC-Na.

7. BIBLIOGRAFÍA

1. Hayashi, J., Kazehaya, A., Muroyama, K., et al., *Preparation of activated carbon from lignin by chemical activation*. Carbon, 2000. **38**(13): p. 1873-1878.
2. Khezami, L., Chetouani, A., Taouk, B., et al., *Production and characterisation of activated carbon from wood components in powder: Cellulose, lignin, xylan*. Powder Technology
4th French Meeting on Powder Science and Technology, 2005. **157**(1-3): p. 48-56.
3. Teng, H., Yeh, T.-S., and Hsu, L.-Y., *Preparation of activated carbon from bituminous coal with phosphoric acid activation*. Carbon, 1998. **36**(9): p. 1387-1395.
4. Gonzalez-Serrano, E., Cordero, T., Rodriguez-Mirasol, J., et al., *Removal of water pollutants with activated carbons prepared from H₃PO₄ activation of lignin from kraft black liquors*. Water Research, 2004. **38**(13): p. 3043-3050.

5. Gonzalez-Serrano, E., Cordero, T., Rodríguez-Mirasol, J., et al., *Development of Porosity upon Chemical Activation of Kraft Lignin with ZnCl₂*. Industrial & Engineering Chemical Research, 1997. **36**(11): p. 4832-4838.
6. Rodríguez-Mirasol, J., Cordero, T., and Rodríguez, J.J., *Preparation and characterization of activated carbons from eucalyptus kraft lignin*. Carbon, 1993. **31**(1): p. 87-95.
7. del Bagno, V.D., Miller, R.L., and Watkins, J.J., *On site production of activated carbon from Kraft Black Liquor*. 1978: U.S.
8. *Activated carbon compendium. A collection of papers from the journal Carbon 1996-2000*. 1ª ed, ed. H. Marsh. 2001, North Shields (UK): Elsevier.
9. Cooney, D.O., *Adsorption design for wastewater treatment*. 1999, Boca Ratón: Lewis Publisher.
10. Lin, S.Y., Jr., S.E.L., and LignoTech USA, I., *Lignin*, in *Kirk-Othmer Encyclopedia of Chemical Technology*. 2000.
11. Lin, S.Y. and Lin, I.S., *Lignin*. Ullmann's Encyclopedia of industrial chemistry, ed. S.H. Barbara Elvers, Gail Schulz. Vol. A15. 1990, New York. 305-315.
12. Hynek, S., Fuller, W., and Bentley, J., *Hydrogen storage by carbon sorption*. International Journal of Hydrogen Energy, 1997. **22**(6): p. 601-610.
13. Das, L.M., *On-board hydrogen storage systems for automotive application*. International Journal of Hydrogen Energy, 1996. **21**(9): p. 789-800.
14. Imamura, H. and Sakasai, N., *Hydriding characteristics of Mg-based composites prepared using a ball mill*. Journal of Alloys and Compounds Proceedings of the International Symposium on Metal-Hydrogen Systems-Fundamentals and Applications, 1995. **231**(1-2): p. 810-814.
15. Imamura, H., Sakasai, N., and Kajii, Y., *Hydrogen absorption of Mg-Based composites prepared by mechanical milling: Factors affecting its characteristics*. Journal of Alloys and Compounds, 1996. **232**(1-2): p. 218-223.
16. Imamura, H., Sakasai, N., and Fujinaga, T., *Characterization and hydriding properties of Mg-graphite composites prepared by mechanical grinding as new hydrogen storage materials*. Journal of Alloys and Compounds, 1997. **253-254**: p. 34-37.
17. Carpetis, C. and Peschka, W., *A study on hydrogen storage by use of cryoadsorbents*. International Journal of Hydrogen Energy, 1980. **5**(5): p. 539-554.
18. Chand Bansal, R., Donnet, J.-B., and Stoeckli, F., *Active Carbon*. 1988, New York and Basel.
19. Chambers, A., Park, C.R., Baker, T.K., et al., *Hydrogen Storage in Graphite Nanofibers*. Journal of Physical Chemistry B, 1998. **102**(22): p. 4253-4256.
20. Dillon, A.C., Jones, K.M., Bekkedahl, T.A., et al., *Storage of hydrogen in single-walled carbon nanotubes*. Nature, 1997. **386**: p. 377-379.

21. *General applications of activated carbon.* in *Ciencia y Tecnología del carbón activo.* 1994. Alicante.
22. Girgis, B.S. and El-Hendawy, A.-N.A., *Porosity development in activated carbons obtained from date pits under chemical activation with phosphoric acid.* *Microporous and Mesoporous Materials*, 2002. **52**(2): p. 105-117.
23. Smisek, M. and Cerny, S., *Active carbon: Manufacture, properties and applications*, ed. Elsevier. 1970, Amsterdam.
24. Rand, B. and Marsh, H., *The process of activation of carbons by gasification with CO₂-III. Uniformity of gasification.* *Carbon*, 1971. **9**(1): p. 79-85.
25. Schafer, H.N.S., *U. S. Patent 4.* 1977. p. 473.
26. Kraehenbuehl, F., Stoeckli, H.F., Addoun, A., et al., *The use of immersion calorimetry in the determination of micropore distribution of carbons in the course of activation.* *Carbon*, 1986. **24**(4): p. 483-488.
27. Suárez-García, F., Martínez-Alonso, A., and Tascón, J.M.D., *Pyrolysis of apple pulp: chemical activation with phosphoric acid.* *J. Annal. Appl. Pyrolysis.*, 2002. **63**(2): p. 283-301.
28. Guo, Y.P., Yang, S.F., Yu, K.F., et al., *The preparation and mechanism studies of rice husk based porous carbon.* *Materials Chemistry and Physics*, 2002. **74**(3): p. 320-323.
29. Qiao, W., Ling, L., Zha, Q., et al., *Preparation of a pitch-based activated carbon with a high specific surface area.* *Journal of Materials Science*, 1997. **32**(16): p. 4447-4453.
30. Sun, J., Rood, M.J., Rostam-Abadi, M., et al., *Natural gas storage with activated carbon from a bituminous coal.* *Gas Separation & Purification Carbon-Based Materials*, 1996. **10**(2): p. 91-96.
31. Hsu, L.-Y. and Teng, H., *Influence of different chemical reagents on the preparation of activated carbons from bituminous coal.* *Fuel Processing Technology*, 2000. **64**(1-3): p. 155-166.
32. Teng, H. and Wang, S.-C., *Preparation of porous carbons from phenol-formaldehyde resins with chemical and physical activation.* *Carbon*, 2000. **38**(6): p. 817-824.
33. Ahmadvour, A. and Do, D.D., *The preparation of activated carbon from macadamia nutshell by chemical activation.* *Carbon*, 1997. **35**(12): p. 1723-1732.
34. Guo, Y.P., Yu, K.F., Wang, Z.C., et al., *Effects of activation conditions on preparation of porous carbon from rice husk.* *Carbon*, 2000. **41**(8): p. 1645-1648.
35. Maciá-Agulló, J.A., Moore, B.C., Cazorla-Amorós, D., et al., *Activation of coal tar pitch carbon fibres: Physical activation vs. chemical activation.* *Carbon*, 2004. **42**(7): p. 1367-1370.
36. Lillo-Rodenas, M.A., Lozano-Castello, D., Cazorla-Amoros, D., et al., *Preparation of activated carbons from Spanish anthracite II. Activation by NaOH.* *Carbon*, 2001. **39**(5): p. 751-759.

37. Lillo-Rodenas, M.A., Cazorla-Amoros, D., and Linares-Solano, A., *Understanding chemical reactions between carbons and NaOH and KOH. An insight into the chemical activation mechanisms*. Carbon, 2003. **41**(2): p. 267-275.
38. Caballero, J.A., Marcilla, A., and Conesa, J.A., *Thermogravimetric analysis of olive stones with sulphuric acid treatment*. Journal of Analytical and Applied Pyrolysis, 1997. **44**(1): p. 75-88.
39. Manya, J.J., Velo, E., and Puigjaner, L., *Kinetics of Biomass Pyrolysis: a Reformulated Three-Parallel-Reactions Model*. Industrial Engineering Chemical Research, 2003. **42**(3): p. 434-441.
40. Orfao, J.J.M., Antunes, F.J.A., and Figueiredo, J.L., *Pyrolysis kinetics of lignocellulosic materials--three independent reactions model*. Fuel, 1999. **78**(3): p. 349-358.
41. Varhegyi, G., Antal, M.J., Szekely, T., et al., *Kinetics of the thermal decomposition of cellulose, hemicellulose, and sugarcane bagasse*. Energy & Fuels, 1987. **3**(3): p. 329-335.
42. Jagtoyen, M. and Derbyshire, F., *Activated carbons from yellow poplar and white oak by H₃PO₄ activation*. Carbon, 1998. **36**(7-8): p. 1085-1097.
43. Montané, D., Torné-Fernández, V., and Fierro, V., *Activated carbons from lignin: kinetic modeling of the pyrolysis of Kraft lignin activated with phosphoric acid*. Chemical Engineering Journal, 2004. **Submitted**.
44. Díaz-Terán, J., Nevskaja, D.M., Fierro, J.L.G., et al., *Study of chemical activation process of a lignocellulosic material with KOH by XPS and XRD*. Microporous and Mesoporous Materials, 2003. **60**(1-3): p. 173-181.
45. Stavropoulos, G.G., *Precursor materials suitability for super activated carbons production*. Fuel Processing Technology, 2005. **86**(11): p. 1165-1173.
46. Park, S.-J. and W.-Y. Jung, *Preparation and structural characterization of activated carbons based on polymeric resin*. Journal of Colloid and Interface Science, 2002. **250**(1): p. 196-200.
47. Guo, Y.P. and Lua, A.C., *Textural and chemical characterization of adsorbent prepared from palm shell by potassium hydroxide impregnation at different stages*. Journal of Colloid and Interface Science, 2002. **254**(2): p. 227-233.
48. Guo, Y.P., Qi, J.R., Yang, S.F., et al., *Adsorption of Cr(VI) on micro- and mesoporous rice husk-based active carbon*. Materials Chemistry and Physics, 2002. **78**(1): p. 132-137.
49. Guo, Y.P., Zhang, H., Tao, N.N., et al., *Adsorption of malachite green and iodine on rice husk-based porous carbon*. Materials Chemistry and Physics, 2003. **82**(1): p. 107-115.
50. Guo, Y.P., Yang, S.F., Fu, W.Y., et al., *Adsorption of malachite green on micro- and mesoporous rice husk-based active carbon*. Dyes and Pigments, 2003. **56**(3): p. 219-229.

51. Lillo-Rodenas, M.A., Juan-Juan, J., Cazorla-Amoros, D., et al., *About reactions occurring during chemical activation with hydroxides*. Carbon, 2004. **Article in press**.
52. www.fao.org/livestock/agap/frg/afris/espanol/document/tfced8/Data/495.HTM, *Madera y subproductos de la madera*.
53. www.fibra-salud.com/.%5CObra%5C9.htm, *Lignina*.
54. Goldstein, I.S., *Productos químicos derivados de la madera*. Unasylva. Chemicals from wood., 1979. **31**(125).
55. www.gtiuruguay.com/lignina.htm, *Lignina*.
56. Northey, R.A. *Low-Cost Uses of Lignin, Emerging Technology of Materials and Chemicals from Biomass*. in *ACS Symposium Series 476*. 1992. Washington D.C.
57. Adler, E., *Lignin chemistry-Past, Present and Future*. Wood Science Technology, 1977. **11**: p. 169-218.
58. Fengel, D. and Wegener, G., eds. *Wood. Chemistry, ultrastructure, reactions*. 1983, Walter de Gruyter: Berlin, New York. 145.
59. Institute, I.L., www.ili-lignin.com/ili_presentation.html. 2005.
60. Goheen, D.W. and Hoyt, C.H., *Lignin*. Third Edition ed. Kirk-Othmer Encyclopedia of Chemical Technology, ed. I. John Wiley & Sons. Vol. 14. 1981, New York: Wiley-Interscience. 294-313.
61. Mansouri, N.-E.E. and Salvado, J., *Structural characterization of technical lignins for the production of adhesives: Application to lignosulfonate, kraft, soda-anthraquinone, organosolv and ethanol process lignins*. Industrial Crops and Products, 2006. **24**(1): p. 8-16.
62. Sarkanen, K.V. and Ludwig, C.H., *Lignins: Occurrence, Formation, Structure and Reactions*. 1971, New York: Wiley-Interscience.
63. Ballerini, A., Ewert, R., and Solís, M., *Utilización de Ligninas en la formulación de adhesivos para tableros contrachapados*. Maderas: Ciencia y Tecnología, 1998. **1**(1).
64. Crawford, D.L., Pometto, A.L., and Crawford, R.L., *Production of useful modified lignin polymers by bioconversion of lignocellulose with Streptomyces*. Biotechnology Advances, 1984. **2**(2): p. 217-232.
65. Mansilla, H., Lizama, C., Gutarra, A., et al., *Tratamiento de residuos líquidos de la industria de celulosa y textil*.
66. Amarasekera, G., Scarlett, M.J., and Mainwaring, D.E., *Development of microporosity in carbons derived from alkali digested coal*. Carbon, 1998. **36**(7-8): p. 1071-1078.
67. Guo, Y. and Rockstraw, D.A., *Physical and chemical properties of carbons synthesized from xylan, cellulose, and Kraft lignin by H₃PO₄ activation*. Carbon, 2006. **44**(8): p. 1464-1475.

68. Fierro, V., Torné-Fernández, V., and Celzard, A., *Highly microporous carbons prepared by activation of Kraft lignin with KOH*. Studies in Surface Science and catalysis, 2005: p. 607-614.
69. *Standard Test Method for methylene blue active substances*, in D3172-89. 2002.
70. Coleman, P.B., *Practical Sampling Techniques for Infrared analysis*. 1993, Boca Raton (EEUU): CRC Press.
71. Muller, M.P. and Griffiths, P.R., *Diffuse reflectance measurements by infrared Fourier transform spectrometry*. Anal. Chem. Vol. 50. 1906-1910.
72. Kendall, D.V., *Applied Infrared Spectroscopy*. 1996: Reinhold Publishing GB.
73. Perkins, W.D., *Fourier Transform- Infrared Spectroscopy*, in *J. Chem. Edu.* 1986. p. A5-A10.
74. Noble, D., *FTIR spectroscopy. It's all done with mirrors*. Anal. Chem. Vol. 6. 1995. 381 A-385 A.
75. Roeges, N.P.G., *Guide to the complete Interpretation of Infrared Spectra of Organic Structures*, ed. C. GB. 1994: John Wiley & Sons.
76. Smith, B., *Infrared Spectral Interpretation. A systematic approach*. 1999, Boca Raton (EEUU): CRC press.
77. Skoog, D.A., Holler, F.J., and Nieman, T.A., *Principios de Análisis Instrumental*. 5ª ed. ed. 2001: McGraw-Hill.
78. Shim, J.-W., Park, S.-J., and Ryu, S.-K., *Effect of modification with HNO₃ and NaOH on metal adsorption by pitch-based carbon fibers*. Carbon, 2001. **39**(11): p. 1635-1642.
79. Oh, G.H. and Park, C.R., *Preparation and characteristics of rice-straw-based porous carbons with high adsorption capacity*. Fuel, 2002. **81**(3): p. 327-336.
80. Moreno-Castilla, C., Carrasco-Marín, F., Maldonado-Hódar, F.J., et al., *Effects of non-oxidant and oxidant acid treatments on the surface properties of an activated carbon with very low ash content*. Carbon, 1998. **36**(1-2): p. 145-151.
81. Chiang, H.-L., Huang, C.P., and Chiang, P.C., *The surface characteristics of activated carbon as affected by ozone and alkaline treatment*. Chemosphere, 2002. **47**(3): p. 257-265.
82. Gregg, S.J., *Adsorption, surface area and porosity*. 1967, London: Academic Press.
83. Lowell, S. and Shield, J.F., *Powder surface area and porosity*, ed. T. Edition. 1979.
84. Rouquerol, F., Rouquerol, J., and Sing, K.S.W., *Adsorption by Powders and Porous Solids. Principles, Methods and Applications*. 1999, San Diego: Academic Press.
85. Kruk, M., Li, Z., Jaroniec, M., et al., *Nitrogen Adsorption Study of Surface Properties of Graphitized Carbon Blacks*. Langmuir, 1999. **15**(4): p. 1435-1441.

86. Tschumper, A. and Prins, R., *Kinetic study of the zeolite catalyzed isomerization of aniline*. Applied Catalysis A: General, 1998. **174**(1-2): p. 129-135.
87. Weeb, P.A., Orr, C., Camp, R.W., et al., *Analytical methods in fine particle technology*. 1997: Micromeritics Instrument Corporation.
88. Setoyama, N., Suzuki, T., and Kaneko, K., *Simulation study on the relationship between a high resolution [alpha]-s-plot and the pore size distribution for activated carbon*. Carbon, 1998. **36**(10): p. 1459-1467.
89. www.vu.union.edu/, *Surface area and pore measurements*.
90. Boehm, H.P., *Some aspects of the surface chemistry of carbon blacks and other carbons*. Carbon, 1994. **32**(5): p. 759-769.
91. Boehm, H.P., *Surface oxides on carbon and their analysis: a critical assessment*. Carbon, 2001. **40**(2): p. 145-149.
92. Contescu, A., Contescu, C., Putyera, K., et al., *Surface acidity of carbons characterized by their continuous pK distribution and Boehm titration*. Carbon, 1997. **35**(1): p. 83-94.
93. Toles, C.A., Marshall, W.E., and Johns, M.M., *Surface functional groups on acid-activated nutshell carbons*. Carbon, 1999. **37**(8): p. 1207-1214.
94. Boehm, H.P., *Chemical Identification of surface groups*. Advances in catalysis, 1966. **16**: p. 179-225.
95. Garten, V.A. and Weiss, D.E., *A new interpretation of the acidic and basic structures in carbons. II. The chromene-carbonium ion couple in carbon*. Australian Journal of Chemistry, 1957. **10**: p. 309.
96. Figueiredo, J.L., Pereira, M.F.R., Freitas, M.M.A., et al., *Modification of the surface chemistry of activated carbons*. Carbon, 1999. **37**(9): p. 1379-1389.
97. Pereira, M.F.R., Soares, S.F., Orfao, J.J.M., et al., *Adsorption of dyes on activated carbons: influence of surface chemical groups*. Carbon, 2003. **41**(4): p. 811-821.
98. *Standard Test Method for methylene blue active substances*, in D 2330 - 02. 2002.
99. Sarmiento, C., Sánchez, J., García, C., et al., *Preparación de carbón activado mediante la activación química de carbón mineral*, in *Ciclo Básico de la Facultad de Ingeniería*: Universidad del Zulia. Maracaibo (Venezuela).
100. Marsh, H., Heintz, E.A., and Rodríguez-Reinoso, F., *Activated carbon: structure, characterization, preparation and applications*, in *Introduction to Carbon Technologies*, S.d.P. Universidad de Alicante, Editor. 1997: Alicante.
101. Rozada, F., Calvo, L.F., Garcia, A.I., et al., *Dye adsorption by sewage sludge-based activated carbons in batch and fixed-bed systems*. Bioresource Technology, 2003. **87**(3): p. 221-230.
102. *Standard Test Method for determination of iodine number of activated carbon*, in D 4607 - 94. 1999.

103. Dabrowski, A., *Adsorption -- from theory to practice*. Advances in Colloid and Interface Science, 2001. **93**(1-3): p. 135-224.
104. El-Hendawy, A.-N.A., *Surface and adsorptive properties of carbons prepared from biomass*. Applied Surface Science, 2005. **252**(2): p. 287-295.
105. Ayranci, E. and Duman, O., *Adsorption behaviors of some phenolic compounds onto high specific area activated carbon cloth*. Journal of Hazardous Materials, 2005. **124**(1-3): p. 125-132.
106. Wu, F.-C. and Tseng, R.-L., *Preparation of highly porous carbon from fir wood by KOH etching and CO₂ gasification for adsorption of dyes and phenols from water*. Journal of Colloid and Interface Science, 2005. **In Press, Corrected Proof**.
107. de Oliveira Pimenta, A.C. and Kilduff, J.E., *Oxidative coupling and the irreversible adsorption of phenol by graphite*. Journal of Colloid and Interface Science, 2005. **In Press, Corrected Proof**.
108. Villacanas, F., Pereira, M.F.R., Orfao, J.J.M., et al., *Adsorption of simple aromatic compounds on activated carbons*. Journal of Colloid and Interface Science, 2005. **In Press, Corrected Proof**.
109. Juang, R.-S., Lin, S.-H., and Cheng, C.-H., *Liquid-phase adsorption and desorption of phenol onto activated carbons with ultrasound*. Ultrasonics Sonochemistry, 2005. **In Press, Corrected Proof**.
110. Khezami, L., Chetouani, A., Taouk, B., et al., *Production and characterisation of activated carbon from wood components in powder: Cellulose, lignin, xylan*. Powder Technology, 2005. **In Press, Corrected Proof**.
111. Otero, M., Zabkova, M., and Rodrigues, A.E., *Adsorptive purification of phenol wastewaters: Experimental basis and operation of a parametric pumping unit*. Chemical Engineering Journal, 2005. **110**(1-3): p. 101-111.
112. Wu, F.-C., Tseng, R.-L., and Hu, C.-C., *Comparisons of pore properties and adsorption performance of KOH-activated and steam-activated carbons*. Microporous and Mesoporous Materials, 2005. **80**(1-3): p. 95-106.
113. Tanthapanichakoon, W., Ariyadejwanich, P., Japthong, P., et al., *Adsorption-desorption characteristics of phenol and reactive dyes from aqueous solution on mesoporous activated carbon prepared from waste tires*. Water Research, 2005. **39**(7): p. 1347-1353.
114. Namane, A., Mekarzia, A., Benrachedi, K., et al., *Determination of the adsorption capacity of activated carbon made from coffee grounds by chemical activation with ZnCl₂ and H₃PO₄*. Journal of Hazardous Materials, 2005. **119**(1-3): p. 189-194.
115. Alvarez, P.M., Garcia-Araya, J.F., Beltran, F.J., et al., *Ozonation of activated carbons: Effect on the adsorption of selected phenolic compounds from aqueous solutions*. Journal of Colloid and Interface Science, 2005. **283**(2): p. 503-512.

116. Wu, F.-C., Tseng, R.-L., and Juang, R.-S., *Comparisons of porous and adsorption properties of carbons activated by steam and KOH*. Journal of Colloid and Interface Science, 2005. **283**(1): p. 49-56.
117. Lee, K.M. and Lim, P.E., *Bioregeneration of powdered activated carbon in the treatment of alkyl-substituted phenolic compounds in simultaneous adsorption and biodegradation processes*. Chemosphere, 2005. **58**(4): p. 407-416.
118. Rio, S., Faur-Brasquet, C., Coq, L.L., et al., *Experimental design methodology for the preparation of carbonaceous sorbents from sewage sludge by chemical activation--application to air and water treatments*. Chemosphere, 2005. **58**(4): p. 423-437.
119. Tancredi, N., Medero, N., Moller, F., et al., *Phenol adsorption onto powdered and granular activated carbon, prepared from Eucalyptus wood*. Journal of Colloid and Interface Science, 2004. **279**(2): p. 357-363.
120. Terzyk, A.P., *Molecular properties and intermolecular forces--factors balancing the effect of carbon surface chemistry in adsorption of organics from dilute aqueous solutions*. Journal of Colloid and Interface Science, 2004. **275**(1): p. 9-29.
121. Nakagawa, K., Namba, A., Mukai, S.R., et al., *Adsorption of phenol and reactive dye from aqueous solution on activated carbons derived from solid wastes*. Water Research, 2004. **38**(7): p. 1791-1798.
122. Roostaei, N. and Tezel, F.H., *Removal of phenol from aqueous solutions by adsorption*. Journal of Environmental Management, 2004. **70**(2): p. 157-164.
123. Nevskaja, D.M., Castillejos-Lopez, E., Guerrero-Ruiz, A., et al., *Effects of the surface chemistry of carbon materials on the adsorption of phenol-aniline mixtures from water*. Carbon, 2004. **42**(3): p. 653-665.
124. Salame, I.I. and Bandosz, T.J., *Role of surface chemistry in adsorption of phenol on activated carbons*. Journal of Colloid and Interface Science, 2003. **264**(2): p. 307-312.
125. Otero, M., Rozada, F., Calvo, L.F., et al., *Elimination of organic water pollutants using adsorbents obtained from sewage sludge*. Dyes and Pigments, 2003. **57**(1): p. 55-65.
126. Tryba, B., Morawski, A.W., and Inagaki, M., *Application of TiO₂-mounted activated carbon to the removal of phenol from water*. Applied Catalysis B: Environmental, 2003. **41**(4): p. 427-433.
127. Podkoscielny, P., Dabrowski, A., and Marijuk, O.V., *Heterogeneity of active carbons in adsorption of phenol aqueous solutions*. Applied Surface Science, 2003. **205**(1-4): p. 297-303.
128. Ariyadejwanich, P., Tanthapanichakoon, W., Nakagawa, K., et al., *Preparation and characterization of mesoporous activated carbon from waste tires*. Carbon, 2003. **41**(1): p. 157-164.

129. Tseng, R.-L., Wu, F.-C., and Juang, R.-S., *Liquid-phase adsorption of dyes and phenols using pinewood-based activated carbons*. Carbon, 2003. **41**(3): p. 487-495.
130. El-Hendawy, A.-N.A., *Influence of HNO₃ oxidation on the structure and adsorptive properties of corncob-based activated carbon*. Carbon, 2003. **41**(4): p. 713-722.
131. San Miguel, Guillermo, Fowler, G.D., and Sollars, C.J., *A study of the characteristics of activated carbons produced by steam and carbon dioxide activation of waste tyre rubber*. Carbon, 2003. **41**(5): p. 1009-1016.
132. Bae, S.-D., Sagehashi, M., and Sakoda, A., *Activated carbon membrane with filamentous carbon for water treatment*. Carbon, 2003. **41**(15): p. 2973-2979.
133. Klimenko, N., Winther-Nielsen, M., Smolin, S., et al., *Role of the physico-chemical factors in the purification process of water from surface-active matter by biosorption*. Water Research, 2002. **36**(20): p. 5132-5140.
134. Chen, X., Jeyaseelan, S., and Graham, N., *Physical and chemical properties study of the activated carbon made from sewage sludge*. Waste Management, 2002. **22**(7): p. 755-760.
135. Galiatsatou, P., Metaxas, M., Arapoglou, D., et al., *Treatment of olive mill waste water with activated carbons from agricultural by-products*. Waste Management, 2002. **22**(7): p. 803-812.
136. Juang, R.-S., Wu, F.-C., and Tseng, R.-L., *Characterization and use of activated carbons prepared from bagasses for liquid-phase adsorption*. Colloids and Surfaces A: Physicochemical and Engineering Aspects, 2002. **201**(1-3): p. 191-199.
137. Laszlo, K. and Szucs, A., *Surface characterization of polyethyleneterephthalate (PET) based activated carbon and the effect of pH on its adsorption capacity from aqueous phenol and 2,3,4-trichlorophenol solutions*. Carbon, 2001. **39**(13): p. 1945-1953.
138. Hu, Z., Srinivasan, M.P., and Ni, Y., *Novel activation process for preparing highly microporous and mesoporous activated carbons*. Carbon, 2001. **39**(6): p. 877-886.
139. Koh, S.-M. and Dixon, J.B., *Preparation and application of organo-minerals as sorbents of phenol, benzene and toluene*. Applied Clay Science, 2001. **18**(3-4): p. 111-122.
140. Juang, R.-S., Wu, F.-C., and Tseng, R.-L., *Mechanism of Adsorption of Dyes and Phenols from Water Using Activated Carbons Prepared from Plum Kernels*. Journal of Colloid and Interface Science, 2000. **227**(2): p. 437-444.
141. Okolo, B., Park, C., and Keane, M.A., *Interaction of Phenol and Chlorophenols with Activated Carbon and Synthetic Zeolites in Aqueous Media*. Journal of Colloid and Interface Science, 2000. **226**(2): p. 308-317.

142. Brasquet, C., Rousseau, B., Estrade-Szwarczkopf, H., et al., *Observation of activated carbon fibres with SEM and AFM correlation with adsorption data in aqueous solution*. Carbon, 2000. **38**(3): p. 407-422.
143. Hsieh, C.-T. and Teng, H., *Influence of mesopore volume and adsorbate size on adsorption capacities of activated carbons in aqueous solutions*. Carbon, 2000. **38**(6): p. 863-869.
144. Koh, M. and Nakajima, T., *Adsorption of aromatic compounds on C_xN-coated activated carbon*. Carbon, 2000. **38**(14): p. 1947-1954.
145. Wu, F.-C., Tseng, R.-L., and Juang, R.-S., *Pore structure and adsorption performance of the activated carbons prepared from plum kernels*. Journal of Hazardous Materials, 1999. **69**(3): p. 287-302.
146. Laszlo, K., Bota, A., Nagy, L.G., et al., *Porous carbon from polymer waste materials*. Colloids and Surfaces A: Physicochemical and Engineering Aspects, 1999. **151**(1-2): p. 311-320.
147. Tai, H.-S. and Jou, C.-J.G., *Application of granular activated carbon packed-bed reactor in microwave radiation field to treat phenol*. Chemosphere, 1999. **38**(11): p. 2667-2680.
148. Hu, Z. and Srinivasan, M.P., *Preparation of high-surface-area activated carbons from coconut shell*. Microporous and Mesoporous Materials, 1999. **27**(1): p. 11-18.
149. Khan, A.R., Ataullah, R., and Al-Haddad, A., *Equilibrium Adsorption Studies of Some Aromatic Pollutants from Dilute Aqueous Solutions on Activated Carbon at Different Temperatures*. Journal of Colloid and Interface Science, 1997. **194**(1): p. 154-165.
150. Khan, A.R., Al-Bahri, T.A., and Al-Haddad, A., *Adsorption of phenol based organic pollutants on activated carbon from multi-component dilute aqueous solutions*. Water Research, 1997. **31**(8): p. 2102-2112.
151. Shu, H.-T., Li, D., Scala, A.A., et al., *Adsorption of small organic pollutants from aqueous streams by aluminosilicate-based microporous materials*. Separation and Purification Technology, 1997. **11**(1): p. 27-36.
152. Warhurst, A.M., McConnachie, G.L., and Pollard, S.J.T., *Characterisation and applications of activated carbon produced from Moringa oleifera seed husks by single-step steam pyrolysis*. Water Research, 1997. **31**(4): p. 759-766.
153. Laszlo, K., Bota, A., and Nagy, L.G., *Characterization of activated carbons from waste materials by adsorption from aqueous solutions*. Carbon, 1997. **35**(5): p. 593-598.
154. Tamon, H., Atsushi, M., and Okazaki, M., *On Irreversible Adsorption of Electron-Donating Compounds in Aqueous Solution*. Journal of Colloid and Interface Science, 1996. **177**(2): p. 384-390.
155. Leng, C.-C. and Pinto, N.G., *Effects of surface properties of activated carbons on adsorption behavior of selected aromatics*. Carbon, 1997. **35**(9): p. 1375-1385.

156. Singh, B., Madhusudhanan, S., Dubey, V., et al., *Active carbon for removal of toxic chemicals from contaminated water*. Carbon, 1996. **34**(3): p. 327-330.
157. Streat, M., Patrick, J.W., and Perez, M.J.C., *Sorption of phenol and para-chlorophenol from water using conventional and novel activated carbons*. Water Research, 1995. **29**(2): p. 467-472.
158. Moreno-Castilla, C., Rivera-Utrilla, J., López-Ramón, M.V., et al., *Adsorption of some substituted phenols on activated carbons from a bituminous coal*. Carbon, 1995. **33**(6): p. 845-851.
159. Nevskaja, D.M., Santianes, A., Munoz, V., et al., *Interaction of aqueous solutions of phenol with commercial activated carbons: an adsorption and kinetic study*. Carbon, 1999. **37**(7): p. 1065-1074.
160. Sabio, E., González-Martín, M.L., Ramiro, A., et al., *Influence of the regeneration temperature on the phenols adsorption on activated carbon*. Journal of Colloid and Interface Science, 2001. **242**: p. 31-35.
161. Wu, F.-C., Tseng, R.-L., Hu, C.-C., et al., *Physical and electrochemical characterization of activated carbons prepared from firwoods for supercapacitors*. Journal of Power Sources, 2004. **138**: p. 351-359.
162. Ghiaci, M., Abbaspur, A., Kia, R., et al., *Equilibrium isotherm studies for the sorption of benzene, toluene, and phenol onto organo-zeolites and as-synthesized MCM-41*. Separation and Purification Technology, 2004. **40**(3): p. 217-229.
163. Basso, M.C. and Cukierman, A.L., *Arundo donax - Based activated carbons for aqueous-phase adsorption of volatile organic compounds*, Programa de investigación y desarrollo de fuentes alternativas de materias primas y energía (PINMATE): Buenos Aires. p. 42.
164. Hindarso, H., Ismadji, S., Wicaksana, F., et al., *Adsorption of benzene and toluene from aqueous solution onto granular activated carbon*. Journal of Chemical and Engineering Data, 2001. **46**(4): p. 788-791.
165. Torras, C., *Obtenció de membranes polimèriques selectives.*, in *Chemical Engineering*. 2005, Universitat Rovira i Virgili: Tarragona.

8. NOMENCLATURA

$\%ML_{P/L}$	Porcentaje de masa pérdida debido a la reacción entre el ácido fosfórico y la lignina
α	Factor de referencia usado en el método α_s
α'	Coefficiente de reacción
α_{LP}	Orden de reacción para la activación de la lignina
α_w	Orden de reacción para transformación de agua
ΔT	Incremento de temperatura ($^{\circ}C$)
μm	Micrómetros

a

AA, AAS	espectroscopía de absorción atómica
AC, ACs	Carbón Activo
AC-K	Carbón activado químicamente con hidróxido de potasio
AC-Na	Carbón activado químicamente con hidróxido de sodio
AC-P	Carbón activado químicamente con ácido fosfórico
ACF	Fibras de carbón activo
AgA	Agente activante
ATD	Análisis térmico diferencial
Atm	Atmósfera utilizada durante el proceso de pirólisis
ATR	Reflexión total atenuada

b

B	Constante de Langmuir referente a la energía de adsorción (l/mg)
BDDT	Codificación según Bruneaur, Deming, Deming y Teller
BET	Teoría de Brunauer-Emmett-Teller

c

$^{\circ}C$	Grados centígrados
C	Cantidad de carbono (%)
C	Normalidad del filtrado residual
$C_{e,j}$	Concentración de la especie j en el equilibrio
$C_{0,j}$	Concentración de soluto en la alimentación
$C_{Se,j}$	Concentración de la especie j adsorbida en la superficie
C_e	Concentración en el equilibrio (mg/l)
C_{LP}	Concentración del complejo lignina-ácido fosfórico
C_{PA}	Concentración de ácido fosfórico

C_{ws}	Concentración de agua
CA	Carbón Activo
CEC	Capacidad de intercambio de cationes (meq/g)

d

$\overline{d_p}$	Diámetro medio de poro
DAD	Detector de diodo
df/dt	Velocidad de reacción de la disminución de la fracción másica inicial restante en el sólido
DFT	Teoría de la densidad funcional
DMF	dimetilformamida
DR	Ecuación de Dubinin-Radushkevich
DRX	Difracción de rayos X

e

E_j	Energía de activación (kJ/mol)
E_o	Energía característica entre el nitrógeno y el carbón (kJ/mol)
EMR	Reactor enzimático de membrana

f

f	Fracción de masa inicial restante en el sólido
f_∞	Fracción de masa inicial restante en el sólido al final de la termogravimetría
f_{ij}^{cal}	Valor calculado de f en un momento i
f_{ij}^{exp}	Valor experimental de f en un momento i
f_{AC}	Fracción de masa inicial de carbón activo restante en el sólido final
f_j	Fracción de másica de la especie j respecto a la masa inicial de la muestra
f_{LP}	Fracción de masa inicial de lignina restante en el sólido final
f_{LPo}	Fracción de masa inicial de lignina en el sólido inicial
f_{PA}	Fracción de masa inicial de ácido fosfórico restante en el sólido final
f_{PO}	Fracción de masa inicial de óxido de fósforo restante en el sólido final
f_w	Fracción de masa inicial de agua restante en el sólido final
f_{ws}	Fracción de masa inicial de vapor restante en el sólido final
F_{wo}	Fracción de masa inicial de agua en el sólido inicial

g

g	Gramos
g_{AC}	Gramos de carbón activado
GA	Gases ligeros
GPC	Cromatografía de permeación de gel

h

h	Adsorción inicial
h	Constante de Freundlich relacionado con la intensidad de adsorción
h	Horas
H	Cantidad de hidrógeno (%)
H	Tipo de carbón con pH básico
HK	Método de Horwath-Kawazoe
HMF	Hidroximetil furfural
HPLC	Cromatografía líquida de alta precisión

i

IMAC	Técnica de cromatografía de afinidad con ión metálico inmovilizado
IR	Espectroscopía de infrarrojo
ISO	International Organization for Standardization
IUPAC	International Union of Pure and Applied Chemistry

k

k	Constante de reacción
k	Parámetro de Langmuir relacionado con la intensidad de adsorción
K	Grados kelvin
K_{0j}	Factor de frecuencia (1/s)
k_b, K_j	Constante de Freundlich relacionado con la capacidad de adsorción
k_{LP}	Constante de Arrhenius para la volatilización de la lignina activada
k_w	Constante de Arrhenius para la volatilización del agua
kDa	Kilodalton
kg	Kilogramo

l

l	litro
L	Lignina
L	Tipo de carbón con pH ácido
Lo	Amplitud media de los microporos (nm)
LK, KL	Lignina Kraft
LK _d	Lignina Kraft desmineralizada
LP	Complejo lignina-ácido fosfórico
LP	Productos derivados de la lignina

m

m	Masa de carbón activado
M	Molaridad (moles/litro)
m _∞	Masa residual al final de la termogravimetría
M ₀	Masa inicial de la muestra
m _{0LP}	Masa inicial de lignina activada
m _{0w}	Masa inicial de agua
m _{1LP}	Masa de lignina activada
m _w	Masa de agua
MB	Azul de metileno
mequiv	Miliequivalentes
mg	Miligramos
min	Minutos
mM	Milimolar
ml, mL	Mililitro
MW _{AC}	Masa molar de carbón activo
MW _j	Masa molar de la especie j
MW _L	Masa molar aparente de la lignina
MW _{PA}	Masa molar de ácido fosfórico
MW _{PO}	Masa molar de óxido de fósforo
MW _{LP}	Masa molar de complejo lignina-ácido fosfórico
MW _{ws}	Masa molar de vapor
MWCO	Peso molecular del cut-off

n

N	Cantidad de nitrógeno (%)
N	Normalidad (equivalentes/litro)
n(i)	Número de puntos

n_i	Constante de Freundlich
nm	Nanómetros
NOC	Componentes orgánicos no iónicos

O

O	Cantidad de oxígeno (%)
---	-------------------------

P

P	Cantidad de fósforo (%)
P/L	Relación másica entre ácido fosfórico y materia prima
P/P ₀	Presión relativa
PA	Ácido fosfórico
PAS	Detector fotoacústico
pH	Concentración de iones [H ⁺]
pH _{PZC}	Potencial de carga cero
pK	Constante de equilibrio ácido-base
PO	Óxido de fósforo
POS	Evaporación de óxido de fósforo
PSD	Distribución de tamaño de poros
PSf	Polisulfona
PVC	Polivinilo clorado

q

Q ₀	Constante de Langmuir referente a la capacidad de adsorción
q _e	Cantidad adsorbida en el equilibrio (mg/g)
Q _{N₂} , f _{N₂}	Cabal de nitrógeno (cm ³ /min)
q _t	Cantidad adsorbida en un tiempo t (mg/g)

r

R	Relación másica entre agente activante y materia prima
r	Velocidad de calentamiento (°C/min)
R _L	Parámetro de equilibrio de Langmuir
rd _j	Reducción de la especie j
RI	Índice refractivo
RID	Detecto de índice refractivo
RMN	Resonancia magnética nuclear
rpm	Revoluciones por minuto
RRIFT	Reflectancia difusa

S

S	Cantidad de azufre (%)
S_{BET}	Área superficial efectiva (m^2/g)
SEM	Microscopía electrónica de barrido

t

t	Tiempo (h ó min)
T	Temperatura ($^{\circ}\text{C}$)
T_a, T_{carb}	Temperatura de activación ($^{\circ}\text{C}$)
TEM	Microscopía electrónica de transmisión
TG	Termogravimetría
T_p, t_{carb}	Tiempo de activación (h)
TPD, TPDR	Desorción a temperatura controlada

U

UV	Ultravioleta
----	--------------

V

V	Volumen
$V_{\text{DR}}, V_{\mu\text{DR}}$	Volumen de microporos calculado según Duvinin-Radushkevich (cm^3/g)
$V_{\text{macroporo}}$	Volumen de macroporos (cm^3/g)
V_{mesoporo}	Volumen de mesoporos (cm^3/g)
$V_{\text{microporo}}$	Volumen de microporos (cm^3/g)
$V_p, V_{0.99}, V_{\text{total}}$	Volumen total de poro (cm^3/g)
$V_{\alpha_{\text{micro}}}$	Volumen de microporo calculado por el método α_s (cm^3/g)
$V_{\alpha_{\text{super}}}$	Volumen de supermicroporo calculado por el método α_s (cm^3/g)
$V_{\alpha_{\text{ultra}}}$	Volumen de ultramicroporo calculado por el método α_s (cm^3/g)
VO	Volátiles

W

W	Agua
WS	Agua evaporada

Z

$\frac{X}{M}$

Índice de iodo

M

x_m

Parámetro de Langmuir relacionado con la máxima capacidad de adsorción (mg/g AC)

XO(s)

Xylo-oligosacárido(s)

XPS

Espectroscopía fotoelectrónica de Rayos X

XRF

Fluorescencia de rayos X

Compuestos químicos

C	Carbono
$C_{16}H_{18}ClN_3S \cdot 2H_2O$	Azul de metileno (cloruro)
CO	Monóxido de carbono
CO ₂	Dióxido de Carbono
Cu (II)	Cobre (II)
$CuCl_2 \cdot 2H_2O$	Cloruro de cobre dihidratado
H ₂	Hidrógeno
HCl	Ácido clorhídrico
H ₂ O	Agua
HPO ₃	Ácido metafosfórico
H ₃ PO ₄	Ácido fosfórico
H ₄ P ₂ O ₇	Ácido pirofosfórico
H _{n+2} P _n O _{3n+1}	Ácido polifosfórico
H ₂ SO ₄	Ácido sulfúrico
He	Helio
I ₂	Yodo
K	Potasio metálico
K ₂ CO ₃	Carbonato de potasio
KNO ₃	Nitrato de potasio
KOH	Hidróxido de potasio
K ₂ O	Óxido de potasio
N ₂	Nitrógeno
Na	Sodio
NaCl	Cloruro de sodio
Na ₂ CO ₃	Carbonato de sodio
NaHCO ₃	Bicarbonato de sodio
Na ₂ O	Óxido de sodio
NaOC ₂ H ₅	Etóxido de sodio
NaOH	Hidróxido de sodio
Na ₂ S	Sulfuro de sodio
Na ₂ SO ₄	Sulfato de sodio
O ₂	Oxígeno
P ₂ O ₅	Óxido de fósforo
Zn	Zinc
ZnCl ₂	Cloruro de zinc

ANEXOS

Anexo A.

Use of Kraft lignin for Cu(II) removal in industrial water.

Anexo B.

Activated carbons prepared from Kraft lignin by phosphoric acid impregnation.

Anexo C.

Removal of Cu (II) from aqueous solutions by adsorption on activated carbons prepared from Kraft lignin.

Anexo D.

Uptake of Cu(II) and Zn from aqueous solution by Kraft lignin.

Anexo E.

Highly microporous carbons prepared by activation of Kraft lignin with KOH.

Anexo F.

Enzymatic composite membranes based on carbon/polysulfone.

Anexo G.

Influence of the ash content on the microporosity of activated carbons derived from Kraft lignin.

ANEXO **A**

**USE OF KRAFT LIGNIN FOR CU (II) REMOVAL IN
INDUSTRIAL WATER.**

9TH MEDITERRANEAN CONGRESS (PÓSTER).

BARCELONA - CATALUNYA (2002).



USE OF KRAFT LIGNIN FOR Cu(II) REMOVAL IN INDUSTRIAL WATER

E. Novellon, V. Fierro*, V. Torné, R. García-Valls, D. Montané

Departament d'Enginyeria Química. Grup de Biopolimers Vegetals. Escola Tècnica Superior d'Enginyeria Química. Universitat Rovira i Virgili. Campus Sescelades 43007 Tarragona, España. e-mail: vfierro@etseq.urv.es Tel. 977558546

The presence of heavy metals in industrial wastewater is one of the major sources of aquatic pollution since they are non biodegradable and accumulate in living tissues, thus becoming concentrated throughout the food chain.

The Kraft process produces a residue call as black liquors composed by lignin (30-40%) and other inorganic compounds, after evaporation black liquors are burnt to recover energy and the remaining inorganic reactants. The separation of kraft lignin could be an alternative to incineration since lignin is a bountiful and renewable resource that can be used as feedstock for the fabrication of complexing agents as it can contain active sites (carboxyl, hydroxyl, sulfonate or amine groups) responsible for the complexation of metal ions.

The purpose of this work is to test the ability of a commercial lignin (Kraft lignin - Curan 1052 provided by Lignotech Ibérica S.A.) as a complexing/adsorption agent to remove copper ions.

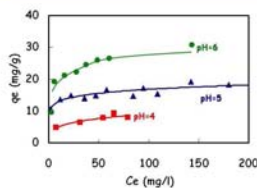
EXPERIMENTAL

150 mg of lignin are added to each 250-ml Erlenmeyer flask containing 150 ml of deionized water. Varying amounts of Cu(II) Chloride (p.a. quality from Aldrich) are added to each flask and maintained under stirring for 24h at 25°C. The resulting Cu(II) concentration is analyzed by atomic absorption (AA). The amount of adsorbed copper is obtained by calculating the difference of each concentration before and after adsorption.



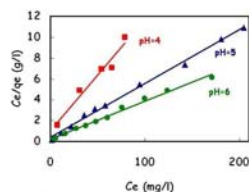
Experimental set up

RESULTS



Maximum Cu(II) removal is obtained at pH=6

q_e (mg/g) equilibrium capacity
 C_e (mg/l) equilibrium concentration
 Q_0 (mg/g) adsorption capacity
 b (l/mg) Langmuir constant
 R_L equilibrium parameter



pH	Q_0 (mg/g)	b (l/mg)	r^2	R_L
4	9.35	0.11	0.96	0.50
5	19.38	0.13	0.99	0.29
6	27.40	0.18	0.99	0.17

Cu(II) removal data fit adequately the Langmuir isotherm

Comparison of adsorption capacity of Cu(II) onto various adsorbents

Adsorbent	Q_0 (mg g ⁻¹)	Reference
Polymerized onion skin	7.55	Kumar et al. 1981
Rice hull	5.58	Suemitsu et al. 1986
Melon seed husk	5.9	Okieman et al. 1989
Red mud	15.0	Zouboulis et al. 1993
Fly ash	0.683	Viswakarma et al. 1989
Ash treated with NaCl	14.54	Hawash et al. 1994
Fe(III)/Cr(III) hydroxide	22.94	Narasivayam et al. 1994
Peanut hull carbon	53.65	Periasamy et al. 1995
Soyabean hull	89.52	Marshall et al. 1995
Bituminous coal	6.47	Singh et al. 1997
<i>Aspergillus niger</i>	1.1	Kapoor et al. 1997
Crab shell	55.88	An et al. 2001
Coirpith carbon	62.5	Kadirvelu et al. 2001
Kraft lignin (pH=6)	27.4	This work

Kraft lignin shows an intermediate capacity for Cu(II) removal

CONCLUSIONS

This study shows that lignin is a good agent for removing Cu(II). As it is used without further modification, its application in the treatment of polluted water could be commercially viable.

ANEXO B

**ACTIVATED CARBONS PREPARED FROM KRAFT
LIGNIN BY PHOSPHORIC ACID IMPREGNATION.**

CARBON (PÓSTER).

OVIEDO – ESPAÑA (2003).



Activated Carbons Prepared from Kraft Lignin by Phosphoric Acid Impregnation

V. Fierro, V. Torne, D. Montané and J. Salvadó

Departament d'Enginyeria Química, ETSEQ, Universitat Rovira i Virgili, Avinguda dels Països Catalans 26, Campus Sescelades, Tarragona 43007, Spain e-mail:vfierro@etseq.urv.es Tel: +34 977 55 85 46 Fax: +34 977 55 85 44

Lignin can be used as precursor for activated carbon as it has been reported on physical activation of eucalyptus Kraft lignin by CO₂ partial gasification¹ and on chemical activation of this precursor by using zinc chloride². However, the use of ZnCl₂ has declined due to the environmental problems³ and phosphoric acid is preferred as activating-dehydrating agent.

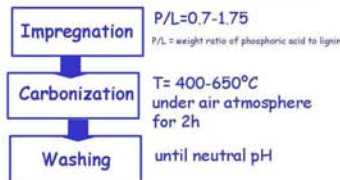
Here we examine the influence of preparation conditions (carbonization temperature, phosphoric-lignin weight ratio and impregnation time) on the carbon yield, surface area and pore size distribution.

EXPERIMENTAL

Lignin Analyses (wt. %)

Proximate (wt. % humid basis)		Elemental (wt. % ash and moisture free)	
Moisture	14.45	Carbon	59.46
Ash	9.50	Hydrogen	5.07
Volatile matter	44.93	Nitrogen	0.05
Fixed carbon*	31.12	Sulfur	2.15
		Oxygen ^b	33.27

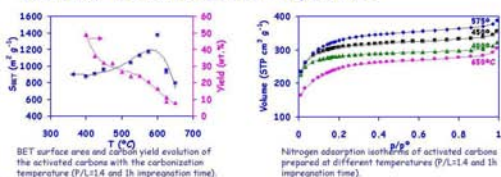
* Estimated by difference



Surface area and pore size characterization were performed using a Micromeritics ASAP2000 gas adsorption surface area analyzer. The specific surface area of the samples was determined from the nitrogen isotherms at -196°C and by using the BET equation. Micropore volume was determined using t-plot, mesopore volume using the BJH equation and total volume of pores was calculated at a relative pressure (p/p⁰) of 0.99.

RESULTS AND DISCUSSION

Effect of the carbonization temperature

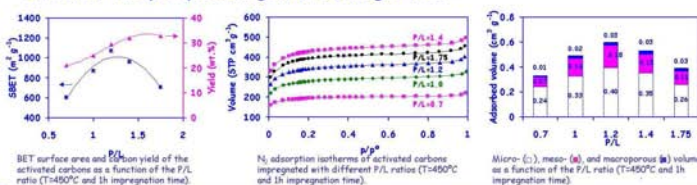


Increasing carbonization temperature carbon yield decreased from 49% at 400°C to 8% at 650°C.

S_{BET} increased between 400 and 600°C, with a maximum of more than 1350m²g⁻¹ at 600°C. At higher temperatures the surfaces areas were considerably reduced.

N₂ isotherms approached type I (Langmuir) with small upward bending at higher pressure, indicating an essentially microporous character with some contribution of wider pores.

Effect of the phosphoric/lignin (P/L) weight ratio

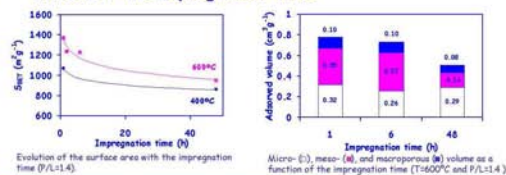


P/L ratio strongly affects the pore structure.

Low P/L ratios promotes the creation of micropores whereas P/L>1.0 slightly affect to the pore size distribution.

P/L ratio has a clear effect on the total volume of pores, there is an optimum for the development of porosity at P/L=1.2.

Effect of the impregnation time



Increasing impregnation times reduces BET surface areas and the total pore volume.

Impregnation time also affects to the pore size distribution of activated carbons.

The effect of impregnation time is more important at high carbonization temperatures due to decomposition of phosphate and polyphosphate bridges crosslinking parts of the carbon structure.

CONCLUSIONS

Pyrolysis of lignin impregnated with phosphoric acid produces essentially microporous activated carbons.

A carbonization temperature of 450°C together with a P/L ratio of 1.2 and low impregnation times produce activated carbons with high specific surfaces areas and reasonable yield.

REFERENCES

- [1] J. Rodríguez-Minazol, T. Cordero, J.J. Rodríguez, Carbon 31 (1993) 87-95.
- [2] E. González Serrano, T. Cordero, J. Rodríguez-Minazol, J.J. Rodríguez Ind. Eng. Chem. Res. 36 (1997) 4832-4838.
- [3] H. Teng, T.S. Yeh, L.Y. Hsu, Carbon 36 (1998) 1387-1395.



ANEXO C

**REMOVAL OF CU (II) FROM AQUEOUS SOLUTIONS BY
ADSORPTION ON ACTIVATED CARBONS PREPARED
FROM KRAFT LIGNIN.**

CARBON (PÓSTER).

OVIEDO - ESPAÑA (2003).



Removal of Cu (II) from Aqueous Solutions by Adsorption on Activated Carbons Prepared from Kraft Lignin

V. Fierro, V. Torne, D. Montané and R. Garcia-Valls

Departament d'Enginyeria Química, ETSEQ, Universitat Rovira i Virgili, Avinguda dels Països Catalans 26, Campus Sescelades, Tarragona 43007, Spain e-mail:vfierro@etseq.urv.es Tel: +34 977 55 85 46 Fax: +34 977 55 85 44

The presence of heavy metals in industrial wastewater is one of the major sources of aquatic pollution since they are non biodegradable and accumulate in living tissues.

This work was undertaken to study the feasibility of the utilization of activated carbon produced from Kraft lignin by chemical activation¹ with phosphoric acid for the removal of heavy metal cations from water solutions. The influence of carbonization temperature and phosphoric acid to lignin weight ratio on Cu adsorption are analyzed.

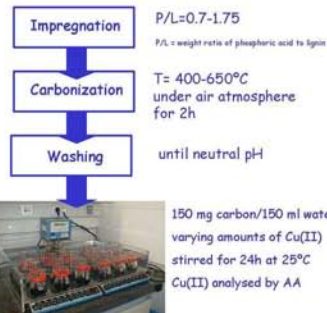
EXPERIMENTAL

Lignin Analyses (wt.%)

Proximate (wt.%, humid basis)		Elemental (wt.%, ash and moisture free)	
Moisture	14.45	Carbon	59.46
Ash	9.50	Hydrogen	5.07
Volatile matter	44.93	Nitrogen	0.05
Fixed carbon*	31.12	Sulfur	2.15
		Oxygen*	33.27

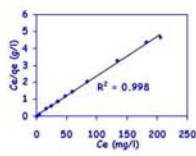
* Estimated by difference

The specific surface area of the carbons was determined from the nitrogen isotherms at 77K and by using the BET equation. Micropore volume was determined using t-plot, mesopore volume using the BJH equation and total volume of pores was calculated at a relative pressure (p/p⁰) of 0.99. Cation exchange capacity (CEC) was measured, after adding NaOH in excess, by titration with HCl and expressed in meq H⁺ g⁻¹.



RESULTS AND DISCUSSION

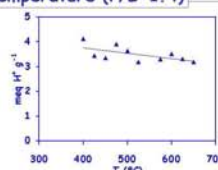
The Langmuir model was applied to the experimental equilibrium data:
 $C_e/q_e = 1/X_m K + C_e/X_m$
 X_m and K are parameters related to the maximum adsorption capacity and intensity of adsorption. X_m was used to study the effect of T and P/L ratio on Cu adsorption. The Langmuir isotherm model describes satisfactorily Cu adsorption on the carbon prepared from Kraft lignin.



Langmuir isotherms for the sorption of Cu on carbon prepared at 450°C and P/L=1.4 (Cu initial concentration: 10-250 ppm)

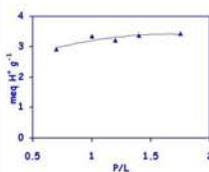
Effect of the carbonization temperature (P/L=1.4)

As temperature increases phosphate and polyphosphate bridges acting as crosslinking parts of the carbon structure decompose and it also could affect to surface phosphorous compounds that are degraded.



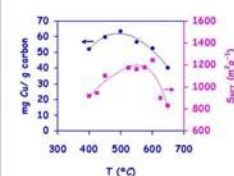
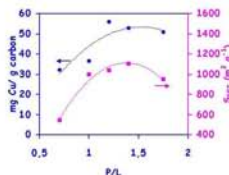
The concomitant effects of T on the CEC and on BET surface explain the existence of a maximum in Cu adsorption for activated carbons prepared at temperatures between 450 and 550°C. At temperatures higher than 600°C, the shrinkage of the structure together with the decreasing tendency of CEC with temperature would explain the Cu adsorption observed.

Effect of the P/L ratio (T = 450°C)



Functional groups increase with P/L ratio but the value remains approximately constant from P/L=1.0. As H₃PO₄ reacts with the hydroxyl groups of lignin it would exist a maximum in the P/L ratio and so a maximum in the phosphorous-containing acids attached to the surface.

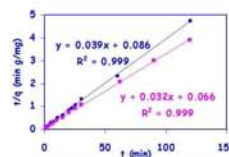
The high CEC together with the no existence of diffusional limitations in carbons at P/L=1.75 explain the slight decrease in copper adsorption even if the surface area decreased greatly from 959 m²g⁻¹ at P/L=1.4 to 704 m²g⁻¹ at P/L=1.75.



Adsorption of Cu on carbon proceeds via a pseudo-second order mechanism

$$t/q_t = 1/h + 1/q_e t$$

where h is the initial sorption, q_e is the equilibrium sorption capacity and the rate constant k can be determined experimentally from the slope and intercept of a plot of t/q_t versus t being $h = k q_e^2$.



Pseudo-second order sorption kinetics for the sorption of Cu²⁺ ions at 300 K and initial concentrations: C₀ = 50ppm; m₀ = C₀ = 100ppm

CONCLUSIONS

Activated carbons produced from Kraft lignin can be tailored to have a high surface concentration of acidic groups and a pore size distribution favorable for adsorption of metallic ions from solutions. Carbonization temperature strongly affects to metal adsorption by changing porosity distribution and degrading phosphorous-acidic groups. The P/L ratio does not influence the amount of copper adsorbed if the added phosphoric acid is enough to allow the complete reaction of lignin.

Pyrolysis of lignin with phosphoric acid at temperatures about 500°C and P/L ratio of 1.0 produces activated carbons with a favorable pore size distribution and enough surface acidic groups for removal of copper ions.

REFERENCES

[1] V. Fierro, V. Torné, D. Montané, J. Salvadó also in Carbon'03, Oviedo (Spain) 2003.



ANEXO D

**UPTAKE OF CU(II) AND ZN FROM AQUEOUS
SOLUTION BY KRAFT LIGNIN.**

**4TH EUROPEAN CONGRESS IN CHEMICAL
ENGINEERING (PÓSTER).**

GRANADA - ESPAÑA (2003).



Uptake of Cu(II) and Zn from Aqueous Solution by Kraft Lignin

G.Nastrunisku, V. Fierro*, V. Torné, R. García-Valls, D. Montané

Departament d'Enginyeria Química, ETSEQ, Universitat Rovira i Virgili, Avinguda dels Països Catalans 26, Campus Sescelades, Tarragona 43007, Spain e-mail:vfierro@etseq.urv.es Tel: +34 977 55 85 46 Fax: +34 977 55 85 44

Kraft lignin (KL) is produced upon wood pulping with a NaOH + Na₂S solution. The lignin fraction of wood is solubilized in chemically modified form, representing the main component of the black liquors, which are separated from cellulose. These black liquors bear a very high pollution load and once concentrated by evaporation, they serve primarily as in-house fuel required for the recovery of chemicals. The separation of KL could be an alternative to incineration since lignin is a bountiful and renewable resource and represents an attractive field for future industrial chemistry.

The presence of heavy metals in industrial wastewater is one of the major sources of aquatic pollution since they are non biodegradable and accumulate in living tissues, thus becoming concentrated throughout the food chain. Therefore, their immobilization is a question of primary interest. Lignin contains active sites (carboxyl, hydroxyl, sulfonate or amine groups) responsible for the complexation of metal ions. The advantages of using lignin are its low toxicity and the re-use of a residue in the production chain, which may reduce pollution levels.

EXPERIMENTAL

Kraft lignin (KL) was provided by Lignotech Iberica S.A. Elemental analysis was carried out in an EA1108 Carlo Erba Elemental Analyzer. The proximate analysis was carried out following ISO standards.

Lignin Analyses (wt.%)

Proximate (wt.%, humid basis)	Elemental (wt.%, ash and moisture free)		
Moisture	14.45	Carbon	59.46
Ash	9.50	Hydrogen	5.07
Volatile matter	44.93	Nitrogen	0.05
Fixed carbon ^a	31.12	Sulfur	2.15
		Oxygen ^a	33.27

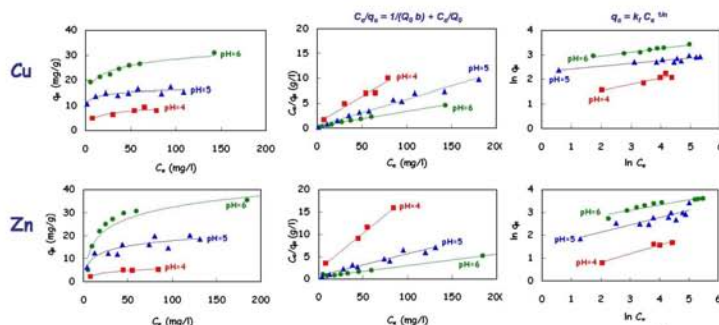
^a Estimated by difference

150 mg of lignin are added to each 250-ml Erlenmeyer flask containing 150 ml of deionized water. Varying amounts of Cu(II) Chloride (p.a. quality from Aldrich) are added to each flask and maintained under stirring for 24h at 25°C. The resulting Cu(II) concentration is analyzed by atomic absorption (AA). The amount of adsorbed copper is obtained by calculating the difference of each concentration before and after adsorption.



Experimental set up

RESULTS AND DISCUSSION



Cu and Zn adsorption onto KL increases with pH from 4 to 6 and the linear plot of q_e/q_m versus C_e showed that both obeys the Langmuir model.

R_L that is defined by

$$R_L = 1 / (1 + b C_0)$$

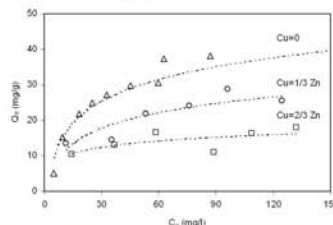
in this study $0 < R_L < 1$ for both metals and at the pH range of this study.

At pH = 6 the maximum Cu(II) removal is of 27.4 mg/g KL whereas reached the maximum Zn removal was 39.22 mg/g lignin. A previous work [1] reported a maximum of Zn²⁺ adsorption of 73.24 mg/g lignin at 30°C but in that case the lignin was intensively purified and washed.

The adsorption did not followed the Freundlich model as well as the Langmuir model. K_f and n were determined. According to Treyball [2], n values between 1 and 10 represents beneficial adsorption. The table shows that n increases with pH and it is always between 1 and 10 for the adsorption of both metals.

pH	Langmuir constants				Freundlich constants			
	Q_0 (mg/g)	b (l/mg)	R_L	R^2	K_f	n	R^2	
Cu	4	9.35	0.11	0.086	0.96	2.82	3.93	0.90
	5	19.38	0.13	0.073	0.99	10.12	4.16	0.89
	6	27.40	0.18	0.053	0.99	14.15	6.57	0.96
Zn	4	6.16	0.08	0.117	0.99	1.04	2.61	0.96
	5	20.37	0.07	0.126	0.94	4.44	3.13	0.80
	6	39.22	0.05	0.155	1.00	11.21	4.42	0.89

q_e (mg/g)	equilibrium capacity	K_f	Freundlich constant related to sorption capacity
C_e (mg/l)	equilibrium concentration	n	Freundlich constant related to the sorption intensity
Q_0 (mg/g)	adsorption capacity		
b (l/mg)	Langmuir constant		
R_L	equilibrium parameter		



Zn adsorbed at equilibrium versus the equilibrium concentration at pH=6 for adsorption of Zn and simultaneous adsorption of Cu and Zn at Cu/Zn (w/w) equal to 1/3 and 2/3.

The data fit adequately de Langmuir adsorption model. The maximum Zn removal when Cu is incorporated to the solution decreases from 39.22 to 32.3 and 19.3 for Cu/Zn (w/w) equal to 1/3 and 2/3 respectively.

CONCLUSIONS

This study shows that lignin is a good agent for removing Cu(II) and Zn. The adsorption of metal depends on pH of the solution and maximum metal uptake is obtained at pH=6. Langmuir and Freundlich parameters shows that Cu(II) and Zn adsorption on KL are favorable. As KL is used without further modification, its application in the treatment of polluted water could be commercially viable.

REFERENCES

- [1] S.K. Srinivastava, A.K. Singh, A. Sharma, *Environmental Technology* 1994, 15, 353.
- [2] R.E. Treybal, *Mass Transfers Operations*, 3rd edn, McGraw, New York, 1980.

ANEXO E

**HIGHLY MICROPOROUS CARBONS PREPARED BY
ACTIVATION OF KRAFT LIGNIN WITH KOH.**

**7TH INTERNATIONAL SYMPOSIUM ON THE
CHARACTERIZATION OF POROUS SOLIDS (PÓSTER).**

AIX-EN-PROVENCE - FRANCIA (2005).

Highly microporous carbons prepared by activation of kraft lignin with KOH



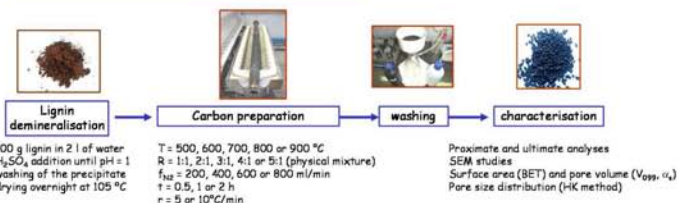
V. Fierro^a, V. Torné-Fernández^a and A. Celzard^b



^a Departament d'Enginyeria Química, Universitat Rovira i Virgili, Campus Sescelades, 43007 Tarragona, Spain
^b Laboratoire de Chimie du Solide Minéral, UMR CNRS 7555, Université Henri Poincaré, 54506 Vandoeuvre-lès-nancy Cédex, France

Highly microporous carbon materials with high apparent BET surface areas (up to ~ 3000 m² g⁻¹) were obtained by heat treatment of mixtures of demineralised kraft lignin (KL_d) and KOH. The effects of five parameters: temperature of activation (T), KOH/KL_d ratio (R), nitrogen flow rate (f_{N₂}), time of activation (t) and heating rate (r) on carbon yield, surface area, pore volume and pore size distribution were investigated.

EXPERIMENTAL



RESULTS

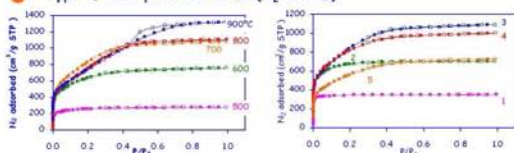
Proximate and ultimate analyses of KL and KL_d (wt. %)

	Proximate Analysis (wt %, dry basis)			Ultimate Analysis (wt %, dry)					
	Fixed Carbon	Volatile matter	ash	C	H	N	S	O*	
KL	36.4	52.5	11.1	59.5	5.1	0.1	2.2	33.3	
KL _d	39.7	60.1	0.2	65.8	5.9	0.0	0.5	27.8	

* Estimated by difference

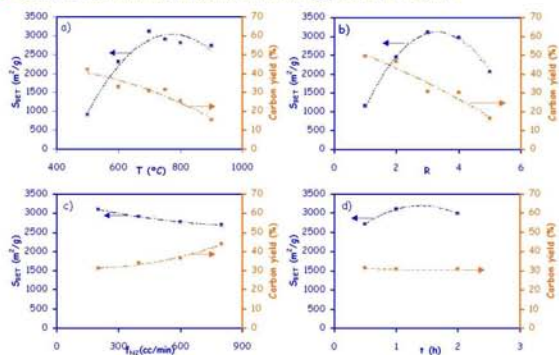
KL has a high ash content, basically Na and Ca combined with S and C inside the phase Na₂CO₃, 2 Na₂SO₄. Lignin demineralisation is very effective: ash content was reduced from 11.1 to 0.2 %.

● Type of adsorption isotherms (N₂ at 77K)



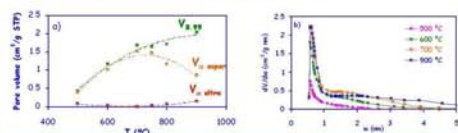
All the isotherms are of type I (Langmuir), characterising microporous solids. Carbons prepared at 500 °C and with R=1 have an essentially microporous character. As T and R increase, the knee of the isotherms widens, indicating a widening of the pores. Carbon prepared at 900 °C shows a hysteresis loop, evidencing a well-developed mesoporosity.

● Effect of activation parameters on both S_{BET} and carbon yield

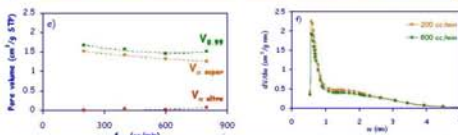


T and R have the most marked effect on both carbon yield and S_{BET}. Increasing the N₂ flow removes part of the activator: carbon yield increases and S_{BET} decreases. The variation of t or r (not shown here) slightly modifies the activated carbon produced.

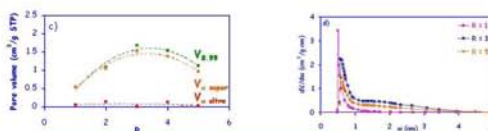
● Effect on both pore volume and pore size distribution



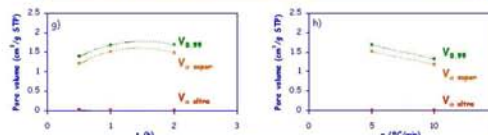
The total pore volume increases with activation temperature but, at temperatures higher than 700 °C, micropores progressively widen to form mesopores.



N₂ flow does not change the PSD but decreases the number of pores.



Pore volumes within the whole pore diameter range are reduced for R > 3; increasing R increases the fraction of wider pores.



1h of activation time is enough to activate the carbon. An increase of the heating rate from 5 to 10 °C/min produces a lowering of the pore volumes.

CONCLUSIONS

- This study evidenced the possibility of preparing highly microporous active carbons from demineralised Kraft lignin, using KOH in suitable experimental conditions.
- The most relevant parameters were found to be activation temperature and mass ratio KOH/lignin. Thus, the best materials (surface area ~ 3000 m²/g, micropore volumes ~ 1.5 cm³/g) were obtained at 700 °C and KOH/KL_d = 3.
- Modifying the experimental conditions easily leads to a range of active carbons, from almost purely microporous to mesoporous.

ANEXO **F**

**ENZYMATIC COMPOSITE MEMBRANES BASED ON
CARBON/POLYSULFONE.**

**ENGINEERING WITH MEMBRANES: MEDICAL AND
BIOLOGICAL APPLICATIONS (PÓSTER).**

CAMOGLI - ITALIA (2005).

Enzymatic composite membranes based on carbon/polysulfone

Carles Torras, Vanessa Torné, Vanessa Fierro, Daniel Montané & Ricard Garcia-Valls

ricard.garcia@urv.net, +34.977.55.96.11



Wood Biopolymers Group
 Department of Chemical Engineering
 Escola Tècnica Superior d'Enginyeria Química
 Universitat Rovira i Virgili
 Av. Països Catalans, 26. 43007 Tarragona (Catalonia - Spain)

Introduction

Versatile materials that have selective properties are of high interest. The objective of these materials is their application in membrane selective reactors. In these reactors, the separation and reaction steps are combined in a single unit. In order to obtain an optimized reactor, the base material (support) is of great importance. In this work, the support is a composite polysulfone membrane that contains activated carbon.

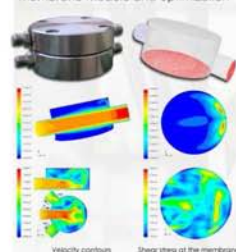
Methods and materials.

- ❖ Membranes. Obtained from Psf (20%w) by immersion precipitation. Solvent: DMF, Non-solvents: IPA & H₂O.
- ❖ Activated carbon. From residual lignin with carbonization at 450°C. Characterized by Micromeritics ASAP 2020. (gas adsorption surface area analyzer).
- ❖ Enzyme. Xylanase (from Sigma-Aldrich), 2.5 u/mg.
- ❖ Fluid: Oligosaccharides from acid hydrolysis of nuts shells up to 40kDa.
- ❖ Experiments carried out in a flat membrane module.

Micromeritics ASAP 2020



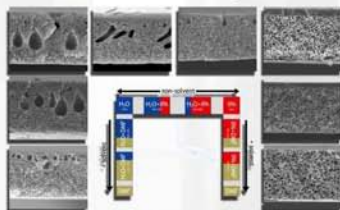
Membrane module and optimization



1. Membranes, activated carbon & composite membranes.

- ❖ Membranes: Cut-off range: 20-600 kDa.
- ❖ Activated carbon. Type I (Langmuir). Microporous character (0.41 cm³/g). BET surface area: 1047 m²/g. Total volume pores: 0.51 cm³/g.
- ❖ Composite membranes. Addition of 0.9% w AC. Membranes morphology & performance do not change.

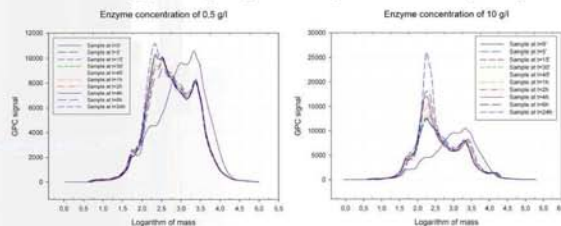
Membrane obtained from several coagulation baths



2. The activity of the enzymes

- ❖ Conditions to obtain chains of 2/3 monomers: Enzyme concentration: low/very low. Reaction time: 0-5'

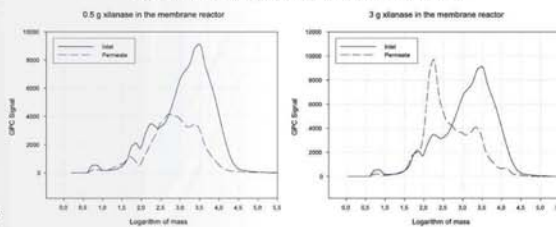
Chromatographs illustrating the degradation of the oligosaccharides due to the enzyme activity



3. The membrane reactor

- ❖ Enzyme was immobilized over the composite membranes.
- ❖ Results show evidence of separation and reaction.
- ❖ With a membrane of 40kDa MWCO and with low amounts of enzyme, a retention of 90% for a sugar size of 17kDa was obtained and also, the permeate contains mainly oligosaccharides of DP=3. This evidences a good equilibrium between the kinetics of the reaction and the separation.
- ❖ With an enzyme concentration too high, the kinetics is not adequate and monomers are mainly obtained.

Chromatographs illustrating the performance of two membrane reactors



Conclusions, references & acknowledgements

- ❖ Activated carbon does not change the morphology and the performance of the membranes.
- ❖ Membranes capable to hold a separation and reaction process have been successfully obtained.
- ❖ Although an optimization should be done, the kinetics of the reactions is consistent with the kinetics of the separation.
- ❖ The immobilization of the enzyme on the carbon-metal complex is in process.
- ❖ C. Torras & R. Garcia-Valls. Quantification of membrane morphology by interpretation of scanning electron microscopy images. *Journal of Membrane Science*, 233 (2004) 119-127.
- ❖ L. Ballinas, C. Torras, V. Fierro & R. Garcia-Valls. Factors influencing activated carbon-polymeric composite membrane structure and performance. *Journal of Physics and Chemistry of Solids*, 65 (2004) 633-637.

C. Torras acknowledges the Rovira i Rovira University for a doctoral scholarship. This work has been supported by the Spanish Ministry of Science and Technology, project PPQ2002-04201-C02.

ANEXO G

**INFLUENCE OF THE ASH CONTENT ON THE
MICROPOROSITY OF ACTIVATED CARBONS DERIVED
FROM KRAFT LIGNIN.**

CARBON (PÓSTER).

COREA (2005).

Influence of the ash content on the microporosity of activated carbons derived from Kraft lignin



Vanessa Fierro^a, Vanessa Torné^a and A. Celzard^b



^a Departament d'Enginyeria Química, Universitat Rovira i Virgili, Campus Sescelades, 43007 Tarragona, Spain
^b Laboratoire de Chimie du Solide Minéral, UMR CNRS 7555, Université Henri Poincaré, 54506 Vandoeuvre-lès-nancy, France

This work focuses on ACs produced from the thermal decomposition of mixtures of orthophosphoric acid (PA) and either as-received Kraft lignin, KL, or demineralised one, KL_d. The yield, surface area and porosity were determined, and the effect of the demineralisation process was investigated.

EXPERIMENTAL

Carbon preparation



RESULTS AND DISCUSSION

	Proximate Analysis (wt %, dry basis)			Ultimate Analysis (wt %, daf)					
	Fixed Carbon	Volatile mat.	ash	C	H	N	S	O*	
KL	36.4	52.5	11.1	59.5	5.1	0.1	2.2	33.3	
KL _d	39.7	60.1	0.2	65.8	5.9	0.0	0.5	27.8	

* Estimated by difference

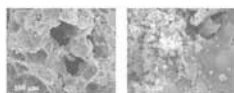
KL has an ash content (11.1% daf basis) that is nearly removed (0.2% daf basis) after the treatment with H₂SO₄.

SEM images of lignins



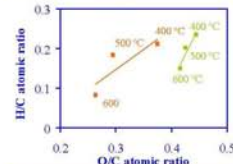
KL particles (left) have a rounded shape with widely open volumes inside. After acid washing, KL_d particles (right) are much bigger and sharp.

SEM images of carbons



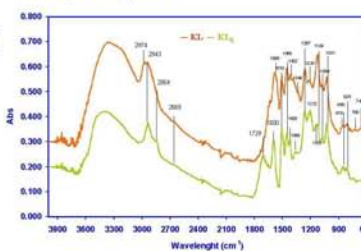
Carbons from KL activated at 400 °C. After carbonisation, the original shape of the particles is lost and a porous structure is revealed.

Van Krevelen diagram



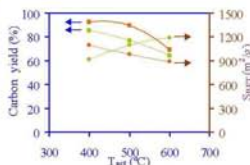
The ACs become more aromatic when T_{act} increases. ACs produced from KL are more aromatic than those from KL_d, and aromaticity increases with T_{act}.

IR analysis of lignins



The most important changes introduced by acid-washing are the reduction of hydroxyl groups and the elimination of carbonates. An intense band in KL_d spectrum centered at 1729 cm⁻¹, which indicates C=O (ketones, aldehydes or carboxyl groups) not associated to aromatic rings, appeared after acid washing.

Carbon yield and S_{BET}

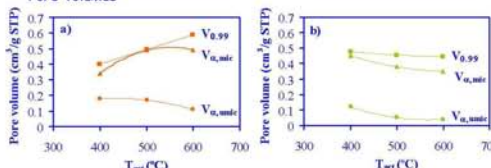


DR model

T (°C)	V _{DR} (cm ³)/(g·mol)	E ₀	L ₀ (nm)
Raw lignin as carbon precursor			
400	0.38	22.2	1.0
500	0.54	19.9	1.3
600	0.51	18.9	1.5
Washed lignin as carbon precursor			
400	0.45	19.1	1.4
500	0.40	17.9	1.7
600	0.37	17.6	1.7

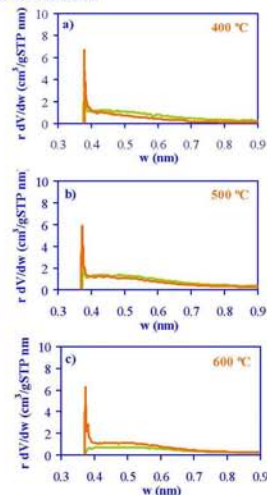
Carbon yield decreases with increasing T_{act} and is always higher for carbons from KL. Opposite evolutions of S_{BET} with T_{act} were found, depending on the precursor. The parameters calculated by applying the DR method are also affected. Carbons from KL_d have a smaller micropore volume, and wider pores.

Pore volumes



ACs from KL_d have higher micropore volumes at 400 °C. However, their pore volumes decrease with increasing T_{act}, contrary to those from KL.

H-K distributions



For ACs from KL, the amount of pores at 0.37 nm is always higher and increases with T_{act}. ACs from KL_d show a wider mean pore size, and a decrease of porosity of width 0.37 nm is observed when ACs were prepared at 600 °C.

CONCLUSIONS

- Carbon yield, surface area, porosity and surface chemistry are affected by the removal of the mineral matter. Carbon yield is higher for activated carbons prepared by activation of the raw Kraft lignin (KL) and such ACs also show a higher aromaticity.
- The activated carbons prepared by activation of KL and demineralised one (KL_d) are essentially microporous with surface areas higher than 800 m²/g. The highest surface area determined in this work, of nearly 1200 m²/g, corresponds to the AC prepared from KL at 600 °C.
- The different characteristics of the ACs are due to the demineralisation process, which produces lignin polymerisation and reduces its ability to react with PA.

NOTAS PARTICULARES

Notas Particulares

Notas Particulares

Notas Particulares

